

REML IMPLEMENTATIONS OF KERNEL-BASED GENOMIC PREDICTION MODELS FOR GENOTYPE \times ENVIRONMENT \times MANAGEMENT INTERACTIONS

KILLIAN A.C. MELSEN^{1*}, SALVADOR GEZAN², DANIEL J. TOLHURST³, FRED A. VAN EEUWIJK¹,
AND CAREL F.W. PEETERS¹

ABSTRACT. High-throughput pheno-, geno-, and envirotyping allows characterization of plant genotypes and the trials they are evaluated in, producing different types of data. These different data modalities can be integrated into statistical or machine learning models for genomic prediction in several ways. One commonly used approach within the analysis of multi-environment trial data in plant breeding is to create linear or nonlinear kernels which are subsequently used in linear mixed models (LMMs) to model genotype by environment (G \times E) interactions. Current implementations of these kernel-based LMMs present a number of opportunities in terms of methodological extensions. Here we show how these models can be implemented in standard software, allowing direct restricted maximum likelihood (REML) estimation of all parameters. We also further extend the models by combining the kernels with unstructured covariance matrices for three-way interactions in genotype by environment by management (G \times E \times M) datasets, while simultaneously allowing for environment-specific genetic variances. We show how the models incorporating nonlinear kernels and heterogeneous variances maximize the amount of genetic variance captured by environmental covariables and perform best in prediction settings. We discuss the opportunities regarding models with multiple kernels or kernels obtained after environmental feature selection, as well as the similarities to models regressing phenotypes on latent and observed environmental covariables. Finally, we discuss the flexibility provided by our implementation in terms of modeling complex plant breeding datasets, allowing for straightforward integration of phenomics, enviromics, and genomics.

Key words: environmental covariates; GBLUP; genomic prediction; genotype-by-environment-by-management interaction; kernel; linear mixed model

1. INTRODUCTION

Genomic prediction has become widespread in the field of plant breeding. In its most basic form, genomic prediction attempts to model genetic estimated breeding values (GEBVs) for quantitative traits as a simple function of genomic single nucleotide polymorphism (SNP) marker scores. The practice of genomic prediction has had a significant impact on the field of plant breeding since its introduction (Meuwissen *et al.*, 2001; Bernardo, 1994). It allows for more efficient allocation of resources within a breeding program and an increased rate of genetic gain by modifying several parameters of the breeder's equation (Eberhart, 1970). Genomic selection, i.e., selection based on GEBVs rather than phenotypes, typically allows for higher selection intensities due to larger populations, higher selection accuracies, and possibly shorter generation intervals (Crossa *et al.*, 2017). A wide variety of models have been used to obtain GEBVs, ranging from machine and deep learning approaches to penalized regression (Pérez-Enciso &

¹MATHEMATICAL & STATISTICAL METHODS GROUP - BIOMETRIS, WAGENINGEN UNIVERSITY & RESEARCH, PO BOX 16, 6700 AA, WAGENINGEN, THE NETHERLANDS

²VSN INTERNATIONAL, 2 AMBERSIDE HOUSE, WOOD LANE, HP2 4TP, HEMEL HEMPSTEAD, UNITED KINGDOM

³THE ROSLIN INSTITUTE AND ROYAL (DICK) SCHOOL OF VETERINARY SCIENCE, UNIVERSITY OF EDINBURGH, EASTER BUSH, MIDLOTHIAN, EH25 9RG, UNITED KINGDOM

E-mail addresses: *killian.melsen@wur.nl.

Zingaretti, 2019; Li & Sillanpää, 2012). Linear mixed models (LMM), however, have long been among the most widely used models due to their ability to model dependencies in the data through random effects, interpretability, and ability to partition observed variance. Instead of direct random regression on genomic SNP scores, LMMs typically include a random effect which is assumed to have a covariance matrix that is proportional to a relationship matrix of genotypes based on pedigree information or the SNP scores themselves (VanRaden, 2008). The LMMs can then be used to obtain predicted breeding values in the form of best linear unbiased predictions (BLUPs) for genotypes, regardless of whether these genotypes were phenotyped in field trials. The models also readily provide estimates of heritabilities which can be used to estimate other quantities like response to selection.

While the LMMs can be used to predict GEBVs within a single trial, in which case it is typically referred to as GBLUP, they are also commonly used to analyze multi-environment trial (MET) data. Here, genotypes are evaluated in several locations and years that together represent a sample of environments from the target population of environments (TPE), i.e., the set of environments targeted by plant breeders (Bančić *et al.*, 2024; Piepho & Williams, 2024; Cooper *et al.*, 2022, 2002). Within environments, co-located trials can be used to evaluate genotypes under a number of different management practices that may be used on farms. Examples of such management practices are rain-fed versus irrigated fields, or fields with different nitrogen fertilization rates. Data obtained from such multi-environment, multi-management trials can be analyzed using LMMs. A commonly used approach is to consider the phenotypes of genotypes under various combinations of managements and environments as different traits in a classical multivariate quantitative genetics framework (Falconer & Mackay, 1996). One key aspect of this approach is that genetic covariances between combinations of managements and environments must typically be estimated from the phenotypic data itself. While the assumption of a simple covariance structure with few parameters can simplify this task, complex, three-way genotype by environment by management ($G \times E \times M$) interactions typically require more flexible structures (Malosetti *et al.*, 2013). However, the parameters underlying these flexible covariance structures can be hard to estimate. This is especially true if genotypes are only evaluated in small subsets of the environments due to an MET design known as *sparse testing* which allows for larger samples of the TPE without increasing the total number of plots (cf. Jarquín *et al.*, 2020).

The increasing use of high-throughput technologies in recent years has provided a possible solution to the problems associated with the estimation of the large numbers of covariance parameters typically required to model MET datasets. The actual number of parameters that need to be estimated can be greatly reduced by replacing unstructured covariance matrices by known similarity matrices based on features obtained from high-throughput technologies. High-throughput methods for characterizing genotypes using SNP markers have been commonly available for a large number of agricultural crops in the past few years. As a result, covariances between genotypes are typically modeled using a product of the previously mentioned relationship matrices and a scalar genetic variance. Recently, cheap sensor technology has made high-throughput characterization of environments possible as well. Weather stations now collect high-resolution longitudinal data on environmental covariables such as temperature, soil water potential, humidity, and solar radiation for every environment within an MET breeding program (Millet *et al.*, 2019). Furthermore, satellite data like those obtained from the NASA POWER (National Aeronautics and Space Administration, Prediction Of Worldwide Energy Resources) project allow environmental characterization of any location on earth (Monteiro *et al.*, 2017). Like for genotypes, these features can easily be used to construct relationship matrices of environments, also referred to as kernels. There has been significant interest in using these types of *enviromics* kernels to model $G \times E$ interactions, resulting in the proposal of several approaches (Costa-Neto *et al.*, 2021a; Crossa *et al.*, 2021; Jarquín *et al.*, 2014; Malosetti *et al.*, 2004).

Among these approaches, (multivariate) reaction norm models using kernels as substitutes for between-environment genetic covariance matrices have been a commonly used choice (Pérez-Rodríguez & de los Campos, 2022; Jarquín *et al.*, 2014; de Los Campos *et al.*, 2010). While the term kernel is used in several contexts in the literature, in the analysis of MET data using LMMs, a kernel typically refers to a positive definite function that produces a Gram matrix of vectors \mathbf{x} and \mathbf{x}' after mapping the vectors from the original space \mathcal{X} to some other space \mathcal{V} . One attractive feature of these kernel methods is the ability to obtain the Gram matrix without performing the explicit mapping $\mathcal{X} \rightarrow \mathcal{V}$. For environments, these vectors contain environmental features derived from covariables that aim to characterize the environment from a crop growth perspective.

Kernel-based models avoid the need to estimate covariance parameters by essentially regressing the phenotypes on products of environmental features and SNP marker scores. They achieve this by assuming that the covariance matrix of the random vector of BLUPs can be expressed as a Kronecker or Hadamard product of appropriately sized and known kernels (Martini *et al.*, 2020; Jarquín *et al.*, 2014). These kernels can be linear, i.e., $\mathcal{X} = \mathcal{V}$, or nonlinear and have been used in a wide variety of models, ranging from support vector machines and other machine learning approaches to the LMMs mentioned above (Costa-Neto *et al.*, 2021a; Keerthi & Lin, 2003). While the use of both linear and nonlinear kernels avoid the need to estimate many covariance parameters, which is especially useful in sparse testing scenarios, an additional benefit of the nonlinear kernels in particular is their flexibility due to the introduction of one or more additional parameters. A commonly used example of such nonlinear kernels is the Gaussian or radial basis function (RBF) kernel which introduces nonlinearity and flexibility through a single parameter often referred to as the bandwidth or scale parameter (Costa-Neto *et al.*, 2021a; Montesinos-López *et al.*, 2021). This flexibility is a result of the so-called *kernel trick* that allows for nonlinearity by mapping the original features, e.g., SNP marker scores or environmental features, to a higher-dimensional space (Montesinos-López *et al.*, 2022; Schölkopf, 2000).

While the mentioned reaction norm models often work well, there are a few opportunities for improving existing implementations. For example, the strategy for selecting an appropriate bandwidth parameter for the Gaussian kernel often relies on cross-validation, Bayesian methods, or a technique known as kernel averaging (Pérez-Elizalde *et al.*, 2015; de Los Campos *et al.*, 2010). Endelman (2011) developed the R-package `rrBLUP` that allows convenient restricted maximum likelihood (REML) estimation of the bandwidth, but only in the context of LMMs with a single genetic variance component, i.e., no $G \times E$ or $G \times E \times M$ interaction models. Finally, the reaction norm models mentioned above estimate a single genetic variance for all environments, thus assuming the same heritability and rate of shrinkage for all environments if a single residual variance is used.

Here, we show how reaction norm models using linear and nonlinear Gaussian kernels for complex $G \times E \times M$ data can be fitted within a frequentist framework using standard LMM software. We also show how the bandwidth parameter of Gaussian kernels can be estimated directly using REML for these interaction models, avoiding the need for slow cross-validation processes. We provide easy-to-use implementations that model heterogeneous genetic variances for all environments, as well as more parsimonious single-variance alternatives, in the form of an R-package. We apply the developed models to two real-world $G \times E \times M$ maize and wheat datasets in a sparse testing context to show the benefits of using kernels and heterogeneous genetic variances in genomic prediction. From an interpretability point of view, we realize that while the environmental features underlying the kernels aim to characterize environments, they cannot perfectly do so. We therefore make use of the LMM's ability to partition genetic variance into kernel and lack of fit components. By doing so, we show that not all $G \times E$ can be predicted from environmental features and that the explanatory power of these features for $G \times E$ interaction variance depends on the management practice following a biologically intuitive pattern.

The remainder of this paper is organized as follows. In section 2 we provide some details on the notation used, a description of the benchmark and kernel-based models, and details on the variance partitioning, cross-validation setup, and software implementation. Section 3 then provides details and results on two publicly available real-world datasets, showing differences between models in terms of variance partitioning and genomic prediction accuracy. We discuss several possible further extensions in Section 4. We conclude in Section 5.

2. METHODS

2.1. Notation. In terms of notation, we denote vectors and matrices with bold lower- and upper-case letters, respectively, while we use normal characters for scalars. Covariance matrices are denoted using $\mathbf{\Sigma}$ while we use \mathbf{R} for correlation matrices. We use subscripts M , E , and G to denote covariance structures related to managements, environments, and genotypes, respectively. For residual covariance matrices and variances we use a sub- or superscript ϵ . We use \mathbf{I}_n for the identity matrix of size n , \mathbf{D} for a distance matrix containing squared Euclidian distances, and \mathbf{K} for a linear kernel, including the genomic relationship or kinship matrix \mathbf{K}_G . The \circ and \otimes operators denote the Hadamard and Kronecker products, and \oplus is used for the direct sum. For a matrix $\mathbf{A} = [a_{ij}]$ we use $\mathbf{B} = e^{\mathbf{A}}$ to define the matrix $\mathbf{B} = [e^{a_{ij}}]$. Finally, let $\text{diag}(\mathbf{a})$ denote the diagonal matrix with elements a_i on the diagonal.

2.2. Modeling approaches. We focus on multi-environment, multi-management trial data, i.e., data containing phenotypic records on multiple genotypes in multiple environments (location-year combinations), and under different management conditions at the same location. Let $\mathbf{y} \in \mathbb{R}^{pqr}$ be the vector of BLUEs (best linear unbiased estimates) for the $G \times E \times M$ combinations where the r genotypes are nested within the q environments, which themselves are nested within p managements:

$$\mathbf{y}^\top = [y_{111} \quad y_{112} \quad \dots \quad y_{ijk} \quad \dots \quad y_{pqr}],$$

where $i = 1, 2, \dots, p$, $j = 1, 2, \dots, q$, $k = 1, 2, \dots, r$, $pqr = n$, and y_{ijk} is thus the phenotype for genotype k in environment j under management i . We use the index $l = 1, 2, \dots, pq$ to iterate over all $E \times M$ combinations. By employing a two-stage modeling approach where individual $E \times M$ combinations are first analyzed to obtain the BLUEs in \mathbf{y} , the data can generally be analyzed in a second stage with LMMs of the following form:

$$(1) \quad \mathbf{y} = \mathbf{X}\boldsymbol{\beta} + \mathbf{Z}\mathbf{u} + \boldsymbol{\epsilon},$$

where $\mathbf{X} \in \mathbb{R}^{n \times pq}$ is a fixed effect design matrix for the means of every $E \times M$ combination and $\boldsymbol{\beta} \in \mathbb{R}^{pq}$ is the vector containing the estimates for these fixed effects. The vector $\boldsymbol{\epsilon} \in \mathbb{R}^n$ contains the residuals which, for all models presented in this paper, are assumed to be independently and identically distributed with mean $\mathbf{0}$ and covariance $\sigma_\epsilon^2 \mathbf{I}_n$. The random effect design matrix $\mathbf{Z} \in \mathbb{R}^{n \times n}$ links records to the nested $G \times E \times M$ BLUPs in \mathbf{u} which have mean zero. It is the modeling of the covariance matrix of this random vector \mathbf{u} that we are primarily concerned with. In a general form this covariance matrix can be represented as

$$\text{Var}(\mathbf{u}) = \boldsymbol{\Sigma}_M \otimes \boldsymbol{\Sigma}_E \otimes \boldsymbol{\Sigma}_G,$$

where $\boldsymbol{\Sigma}_M$ is the between-managements genetic covariance matrix, $\boldsymbol{\Sigma}_E$ is the between-environments genetic covariance matrix, and $\boldsymbol{\Sigma}_G$ is a matrix containing additive genetic relationships between genotypes. Note that $\boldsymbol{\Sigma}_G$ may be a pedigree-based relationship matrix \mathbf{A}_G . For the remainder of this paper, however, we will assume that $\boldsymbol{\Sigma}_G$ is the SNP-based additive genomic relationship matrix \mathbf{K}_G , which is a linear kernel. Table 1 provides an overview of the benchmark and kernel-based models that are described in the remainder of this section in terms of the number of parameters underlying the covariance structures. Figure 1 provides a graphical overview of the different kernel-based models. We start by describing the benchmark additive

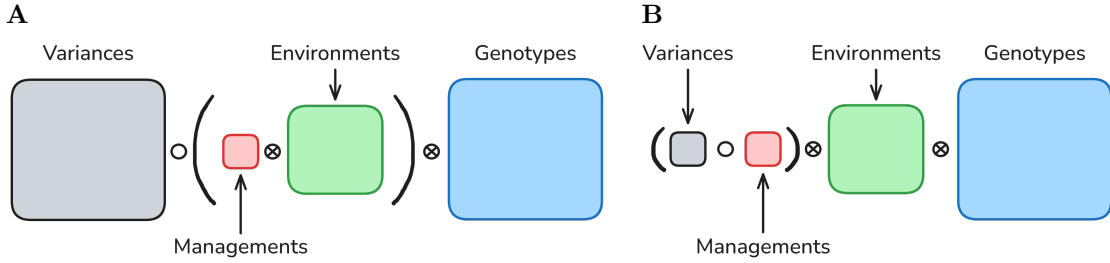


FIGURE 1. Graphical representation of the different kernel-based $G \times E \times M$ covariance structures. For the multiple variance models (**A**), the unstructured correlation matrix for managements (red) is first combined with the kernel for environments (green) and expanded to all $E \times M$ combinations before multiplication with the environment-specific variances (gray). For the single variance models (**B**), variances are first multiplied with the unstructured correlation matrix for managements before forming the Kronecker product with the kernel for environments. Both the single and multiple variance models finally involve a second Kronecker product with the kinship matrix (blue). Note that the kernel for the environments may be linear or nonlinear.

main effect and factor analytic models in Sections 2.2.1 and 2.2.2, followed by four different kernel-based models of increasing complexity.

2.2.1. *Additive main effects (ADD)*. The baseline model contains a random effect for the genotypes only, thus treating all $E \times M$ combinations as if they were perfectly genetically correlated. As a result, the dimensions of \mathbf{Z} and \mathbf{u} for the ADD models differ slightly from those given for the general model (1). For the main effects model, $\mathbf{Z} \in \mathbb{R}^{n \times r}$ links BLUEs in \mathbf{y} to BLUPs in $\mathbf{u} \in \mathbb{R}^r$. This means the model produces a single BLUP for every genotype and the covariance of \mathbf{u} is modeled as

$$\text{Var}(\mathbf{u}) = \sigma^2 \mathbf{K}_G,$$

where σ^2 is the additive genetic variance.

2.2.2. *Order m factor analytic (FA- m)*. The factor analytic (FA) models of different orders form the benchmark interaction models. FA models include $G \times E \times M$ interactions by using the phenotypic data to estimate genetic correlations. They are a more parsimonious alternative to fully unstructured models that typically cannot be fitted on datasets with more than a few environments (Butler *et al.*, 2023; Tolhurst *et al.*, 2019). FA models usually collapse the management and environment factors into a new factor with pq levels for three-way $G \times (E \times M)$ interactions. This factor is subsequently modeled using loadings $\mathbf{\Lambda} \in \mathbb{R}^{pq \times m}$ and unique variances $\mathbf{\Psi} = \text{diag}(\psi)$ for each $E \times M$ combination, given a number of latent factors m :

$$\text{Var}(\mathbf{u}) = (\mathbf{\Lambda} \mathbf{\Lambda}^\top + \mathbf{\Psi}) \otimes \mathbf{K}_G.$$

Each $E \times M$ combination is thus modeled using a unique additive genetic variance, and genomic predictions are obtained for all $E \times M$ combinations for which phenotypic data are available.

2.2.3. *Single variance linear kernel (SV-LK)*. The standard multivariate reaction norm model essentially regresses phenotypes on the products of environmental features obtained from covariables and SNP marker scores using a single genetic variance for each level of management (Pérez-Rodríguez & de los Campos, 2022; Jarquín *et al.*, 2014; de Los Campos *et al.*, 2010). Literature on reaction norm models typically uses notation involving Hadamard products:

$$(2) \quad \text{Var}(\mathbf{u}) = \mathbf{Z}_M \mathbf{\Sigma}_M \mathbf{Z}_M^\top \circ \mathbf{Z}_E \mathbf{K}_E \mathbf{Z}_E^\top \circ \mathbf{Z}_G \mathbf{K}_G \mathbf{Z}_G^\top,$$

where $\mathbf{Z}_M \in \mathbb{R}^{n \times p}$, $\mathbf{Z}_E \in \mathbb{R}^{n \times q}$, and $\mathbf{Z}_G \in \mathbb{R}^{n \times r}$ are design matrices linking records to managements, environments, and genotypes, and $\boldsymbol{\Sigma}_M$ is an unstructured genetic covariance matrix for the p levels of managements. Environmental features are used to construct the linear kernel for environments \mathbf{K}_E :

$$(3) \quad \mathbf{K}_E = \frac{\mathbf{W}^\top \mathbf{W}}{s - 1},$$

where $\mathbf{W} \in \mathbb{R}^{s \times q}$ is a column-wise scaled and centered matrix containing s features obtained from environmental covariables for q environments that have also been scaled and centered to ensure quantities measured in different units have comparable scales. The linear kernel \mathbf{K}_E is thus a correlation matrix, meaning that the implicit mapping underlying the kernel is the identity map (Costa-Neto *et al.*, 2021a). Additive genetic relationships between genotypes are given by \mathbf{K}_G . Note that in this formulation, unique additive genetic variances σ_i^2 are only estimated for every management level i , not every E×M combination l , even if phenotypic data are available for all environments. Also note that if the data are balanced, i.e., there are exactly $n = pqr$ records in \mathbf{y} , and ordered so that genotypes are nested within environments within managements, the notation using Hadamard products in (2) can be freely exchanged with notation using Kronecker products (Martini *et al.*, 2020):

$$(4) \quad \text{Var}(\mathbf{u}) = \boldsymbol{\Sigma}_M \otimes \mathbf{K}_E \otimes \mathbf{K}_G.$$

2.2.4. Multiple variance linear kernel (MV-LK). This model extends the previous covariance model (4) with unique variances for each combination of environment and management, allowing for environment-specific rates of shrinkage. This results in the following covariance matrix for \mathbf{u} :

$$\text{Var}(\mathbf{u}) = \mathbf{s}\mathbf{s}^\top \circ (\mathbf{R}_M \otimes \mathbf{K}_E) \otimes \mathbf{K}_G,$$

where \mathbf{R}_M is an unstructured correlation matrix of managements. The linear kernel \mathbf{K}_E and genomic relationship matrix \mathbf{K}_G are as described before. The column vector \mathbf{s} of length pq contains the additive genetic standard deviations for each E×M combination.

2.2.5. Single variance Gaussian kernel (SV-GK). The next model is a REML implementation of the Gaussian kernel based on environmental covariables for the environments. While the previous two kernel-based models relied on a linear kernel, and thus implied an identity map resulting in a regression of phenotypes directly on the original environmental features, the last two kernel models use nonlinear, Gaussian kernels. The Gaussian kernel $e^{-h\mathbf{D}}$, also referred to as the radial basis function (RBF) kernel, implies a mapping to infinite-dimensional space (Ring & Eskofier, 2016; Vert *et al.*, 2004). While regression on an infinite number of features is clearly impractical, the Gaussian kernel is easily implemented in a LMM through the *kernel trick* by assuming the following covariance structure (Montesinos-López *et al.*, 2022; Schölkopf, 2000):

$$(5) \quad \text{Var}(\mathbf{u}) = \boldsymbol{\Sigma}_M \otimes e^{-h\mathbf{D}_E} \otimes \mathbf{K}_G,$$

where the symmetric matrix \mathbf{D}_E contains squared Euclidian distances between environments. The parameter $h \in (0, \infty)$ is the bandwidth determining the nonlinear transformation of squared Euclidian distances to correlations (Figure 2). The bandwidth thus introduces flexibility resulting in a model that is expected to fit the data better than the simpler linear kernel-based models (Montesinos-López *et al.*, 2021). The distances are computed by averaging the squared differences between features obtained from environmental covariables for environment j and j' :

$$(6) \quad \mathbf{D}_{E_{jj'}} = \frac{1}{s} \sum_{b=1}^s (\mathbf{W}_{bj} - \mathbf{W}_{bj'})^2,$$

where $\mathbf{W} \in \mathbb{R}^{s \times q}$ contains the s features for q environments and is row-wise centered and scaled. Note that $\mathbf{D}_{E_{jj'}} = 0$ if $j = j'$.

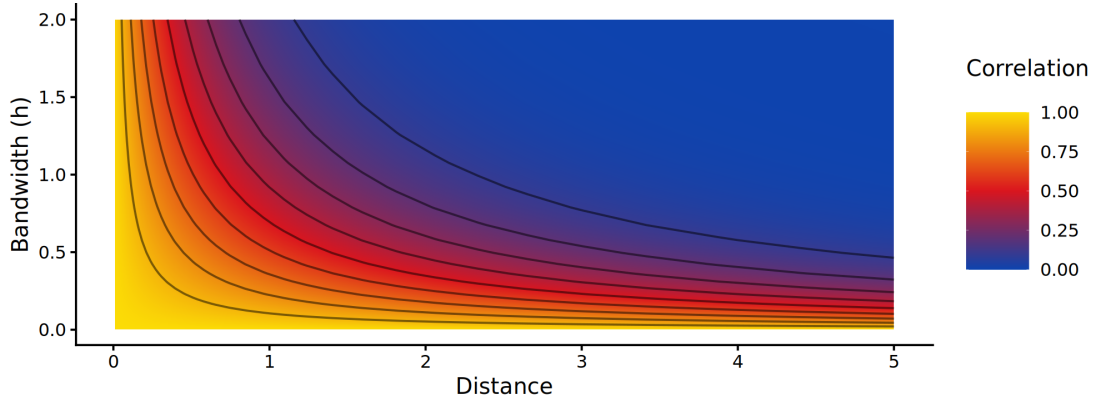


FIGURE 2. The Gaussian kernel nonlinearly transforms squared Euclidian distances between environments to genetic correlations, with the transformation depending on the bandwidth parameter $h \in (0, \infty)$. Genetic correlations tend to 0 for large bandwidth values, regardless of the distance, while for small bandwidth values the opposite is true. Black contour lines are placed at 0.1 intervals.

TABLE 1. Overview of the models described in Section 2.2. ADD = additive main effects, FA- m = order m factor analytic, SV-LK = single variance linear kernel, MV-LK = multiple variance linear kernel, SV-GK = single variance Gaussian kernel, MV-GK = multiple variance Gaussian kernel. Note that the $(m^2 - m)/2$ constrained loadings have been subtracted for the FA models.

Model	$\text{Var}(\mathbf{u})$	Number of parameters for $\text{Var}(\mathbf{u})$
ADD	$\sigma^2 \mathbf{K}_G$	1
FA- m	$(\mathbf{\Lambda} \mathbf{\Lambda}^\top + \mathbf{\Psi}) \otimes \mathbf{K}_G$	$pqm + pq - (m^2 - m)/2$
SV-LK	$\mathbf{\Sigma}_M \otimes \mathbf{K}_E \otimes \mathbf{K}_G$	$(p^2 + p) / 2$
MV-LK	$\mathbf{ss}^\top \circ (\mathbf{R}_M \otimes \mathbf{K}_E) \otimes \mathbf{K}_G$	$pq + (p^2 - p) / 2$
SV-GK	$\mathbf{\Sigma}_M \otimes e^{-h\mathbf{D}_E} \otimes \mathbf{K}_G$	$(p^2 + p) / 2 + 1$
MV-GK	$\mathbf{ss}^\top \circ (\mathbf{R}_M \otimes e^{-h\mathbf{D}_E}) \otimes \mathbf{K}_G$	$pq + (p^2 - p) / 2 + 1$

2.2.6. *Multiple variance Gaussian kernel (MV-GK)*. The final model then extends (5) with unique genetic variances for all combinations of environments and managements, combining the flexibility of the Gaussian kernel with environment-specific rates of shrinkage:

$$\text{Var}(\mathbf{u}) = \mathbf{ss}^\top \circ (\mathbf{R}_M \otimes e^{-h\mathbf{D}_E}) \otimes \mathbf{K}_G,$$

where \mathbf{s} again contains additive genetic standard deviations for all $E \times M$ combinations.

2.3. **Implementations.** The following three subsections provide details on the implementations of models for $G \times E \times M$ variance partitioning, the cross-validation setup for evaluating genomic prediction accuracy, and software.

2.3.1. *Variance partitioning.* Our initial interest was the separation of $G \times E \times M$ interaction variances into components explained by a structured random effect such as the kernels or FA structures and components explained by diagonal lack of fit (LOF) effects. To do so, we fitted a random effect with diagonal covariance structure on $E \times M$ combinations in addition to the kernel-based random effects described in Section 2.2. These models are identifiable due to the structure imposed by the linear kernel \mathbf{K}_E or distance matrix \mathbf{D}_E . Summing these two independent random effects produces the following covariance model:

$$(7) \quad \text{Var}(\hat{\mathbf{u}}) = \text{Var}(\mathbf{u}) + \text{Var}(\mathbf{u}_{LOF}) = \mathbf{\Omega} + \bigoplus_{l=1}^{pq} \sigma_l^2 \mathbf{K}_G,$$

where $\mathbf{\Omega}$ is one of the SV-LK, SV-GK, MV-LK, or MV-GK covariance structures described in Section 2.2 and $\bigoplus_{l=1}^{pq} \sigma_l^2 \mathbf{K}_G$ corresponds to the random LOF effect capturing the $G \times E \times M$ variances not explained by the environmental covariables for each $E \times M$ combination l . The LOF term additionally captures variance not captured by the kernel due to the fact we use a separable structure for the $E \times M$ interactions. This separable structure assumes the correlation between any pair of environments is equal for all managements. While limiting in some sense, this assumption allows us to separate environment and management effects even if they are fully confounded.

We also fitted factor analytic models of orders 1, 2, and 3 where we regarded the diagonal elements of $\mathbf{\Lambda}\mathbf{\Lambda}^\top$ as variances captured by the structured effect, i.e., latent environmental covariables, and the diagonal elements of $\mathbf{\Psi}$ as LOF variances.

Finally, we fitted a benchmark model containing an additive main effect and lack of fit term which is equivalent to the MDe model described by Bandeira e Sousa *et al.* (2017). Note that Bandeira e Sousa *et al.* (2017) use the term deviation where we use lack of fit. Also note that while this model contains both a main effect and interaction term, no correlations between environments or managements are estimated. In fact, the main effect assumes correlations between all $E \times M$ combinations are 1 and the covariance matrix of the interaction term is a Kronecker product of a heterogeneous diagonal covariance structure for $E \times M$ combinations and a kinship matrix, which is equivalent to $\text{Var}(\mathbf{u}_{LOF})$ as described in (7).

2.3.2. *Cross-validation setup for sparse testing genomic prediction.* We evaluated genomic prediction accuracy of the different models described in Section 2.2 in sparse testing scenarios where the missing $G \times E \times M$ combinations had to be predicted. The level of sparsity was varied by sampling increasingly large groups of genotypes which were considered as checks, i.e., genotypes for which phenotypic data from all environments and managements were available. The remaining genotypes had phenotypic data from only 2 environments and, together with the checks, formed the training set. The training sets were sampled such that the same number of training records was available for each $E \times M$ combination. The test set thus consisted of the combinations of genotypes, managements, and environments for which phenotypic data were missing. Performance was evaluated for each $E \times M$ combination in terms of correlation and root mean squared error (RMSE) between BLUPs from the LMMs and centered test set phenotypes (Runcie & Cheng, 2019).

2.3.3. *Software.* All models were implemented using `ASReml-R` version 4.2 (Butler *et al.*, 2023). We used either 1, 2, or 3 factors for the FA models. The kernel-based models were implemented using `ASReml-R`'s `own()` function which requires partial derivatives of the covariance matrices with respect to all parameters for the product of managements and environments. Information on the use of `own()` as well as expressions for the partial derivatives can be found in the Appendix. Functions facilitating the implementation of the kernel-based models for $G \times E$ and $G \times E \times M$ data using `ASReml-R` are provided in the R-package `cornfruit` available at <https://github.com/KillianMelsen/cornfruit>. Scripts and data to reproduce the presented results are available at https://github.com/KillianMelsen/kernels_2026.



FIGURE 3. The locations of field trials in the Briwecs (A) and DROPS (B) datasets after subsetting to a balanced set of records. The DROPS location Graneros (Gra), Chile is not shown.

3. ILLUSTRATIONS

We used two publicly available real-world datasets, one on wheat and one on maize, to illustrate the performance and variance partitioning of the different $G \times E \times M$ models described in the previous section.

3.1. BRIWECS. The first $G \times E \times M$ dataset we used to illustrate performance of the different models is the BRIWECS dataset (Breeding innovations in wheat for efficient cropping systems, (Wang *et al.*, 2025)). It contains measurements on yield, among other traits, for 6 locations in Germany during 2015-2020 for 228 genotypes. In each environment (location-year), up to 9 management practices were evaluated in independent co-located trials. We used the 135K SNP markers published by Lichthardt *et al.* (2019) to compute a genomic relationship matrix using the `statgenGWAS` R-package (identity by state method and minor allele frequency threshold of 0.05) after recoding using the `ASRgenomics` R-package (van Rossum & Kruijjer, 2025; Gezan *et al.*, 2022). We randomly sampled 250 training and test sets for the sparse testing genomic prediction scenarios.

3.1.1. Pre-processing of phenotypic data. We used a subset of the full dataset for our analyses to ensure we had a fully balanced dataset that could be used for evaluating different degrees of sparsity. We initially considered the years 2015-2017 and the LN_NF_RF, HN_NF_RF, L_WF_RF, and HN_WF_RF managements. In the abbreviations for the managements, LN/HN stand for low and high nitrogen, NF/WF for trials without and with fungicide applications, and RF for rain-fed. We then discarded the RHH_2017, GGE_2015, GGE_2016, and GGE_2017 environments. RHH_2017 had data for only 50 genotypes and GGE_2015, GGE_2016, and GGE_2017 had data for only a single management.

We then fitted first stage, single-trial models to the remaining 14 environments to obtain BLUEs using the R-package `LMMsolver` (Boer, 2023):

$$y_{ikuvw} = \mu + g_{ik} + b_{iu} + r_v + c_w + f_{vw}(r, c) + \epsilon_{ikuvw},$$

where g_{ik} is a nested fixed effect for each genotype k within each management i , $b_{iu} \sim \mathcal{N}(0, \sigma_b^2)$ is a random effect for each management-block combination, and $r_v \sim \mathcal{N}(0, \sigma_r^2)$ and $c_w \sim \mathcal{N}(0, \sigma_c^2)$ are random effects for the row and column. Spatial trends across rows and columns are modeled by the smooth surface $f(r, c)$ (Rodríguez-Álvarez *et al.*, 2018). The overall intercept is given by μ and $\epsilon_{ikuvw} \sim \mathcal{N}(0, \sigma_\epsilon^2)$ is the residual. See (Wang *et al.*, 2025) for more details on the

experimental design of individual trials. BLUEs for each management-genotype combination for the second stage $G \times E \times M$ analyses were then obtained as $\bar{y}_{ik} = \mu + g_{ik}$. We subset these BLUEs to those corresponding to the LN_NF_RF and HN_NF_RF managements, i.e., rain-fed trials with low and high nitrogen, no fungicide application, for a total of 28 $E \times M$ combinations. We finally discarded any genotypes that were not evaluated in all 28 $E \times M$ combinations, resulting in a final balanced dataset of 5656 BLUEs for 202 genotypes.

3.1.2. Pre-processing of environmental data and kernels. We used the NASA POWER database and R-package `EnvRtype` to obtain environmental covariables for all 14 environments (Costa-Neto *et al.*, 2021b). This requires geographical coordinates, as well as start and end dates for the period over which data will be retrieved. We used the average sowing and harvest dates for each environment to define the periods. Four environments had missing harvest dates. We computed the average trial duration using the other 10 environments and used this average combined with the sowing dates to obtain estimated harvest dates for the four environments. We kept 18 of the environmental covariables obtained from POWER, including covariables related to precipitation, solar radiation, and temperature. See Table S1 for the geographical coordinates, sowing and harvest dates, and environmental covariables we used to compute the kernels.

We transformed the time-axis of the obtained covariables from days after sowing to thermal time (τ , growing degree days) using the following formula (North Dakota Agricultural Weather Network, 2025a):

$$(8) \quad \tau_a = \frac{T_{min|a} + T_{max|a}}{2} - 32,$$

where the thermal time τ on day a is computed using the minimum and maximum temperatures of that day and a base temperature of 32 degrees Fahrenheit. If $T_{min|a}$ or $T_{max|a}$ were below 32 or above 95, the values were set to the minimum and maximum temperatures of 32 or 95, respectively. We then scaled and centered the environmental covariables before computing the mean value for every covariable for windows of 100 accumulated growing degree days. These means were then used as features to compute the kernels using (3) and (6).

3.1.3. Results. We initially fitted LMMs to investigate the partitioning of variance as described in Section 2.3.1. For the BRIWECS data, narrow-sense heritabilities considering the total genetic variance, i.e., the sum of genetic variances captured by the structured and LOF effects, were reasonably high at average values of 0.91 for the high nitrogen management and 0.85 for the low nitrogen management. While the original paper describing the data did not include any estimates for heritabilities, a publication on a similar $G \times E$ dataset on historic wheat cultivars evaluated in Germany and northern France reported high heritabilities as well (Gogna *et al.*, 2022). Total genetic variance was consistently higher in the high nitrogen management (94.96 averaged over the different models and environments, excluding the ADD model) compared to the low nitrogen management (54.99). There is a clear trend for the percentage of genetic variance explained by the environmental covariables when moving from the most parsimonious to the most complex model (Figure 4). Averaged over environments and managements, the covariables explain 75% of the genetic variance when using the single variance linear kernel, 83% when using the multiple variance linear kernel, 83% for the single variance Gaussian kernel, and 87% for the multiple variance Gaussian kernel. There is a similar trend for the factor analytic models where the percentage of genetic variance explained by the latent environmental covariables increases from 71% for the FA-1 model, to 76% for the FA-2 model and finally 81% for the FA-3 model. For the ADD benchmark model the percentage of genetic variance explained by the main effect is low at 46%. Introducing the additional flexibility of the Gaussian kernel and environment-specific rates of shrinkage thus increases the explanatory power of the environmental covariables. Charts showing the variance partitioning for individual environments can be found in Figure S1 and S2 of the Supplementary Material (SM).

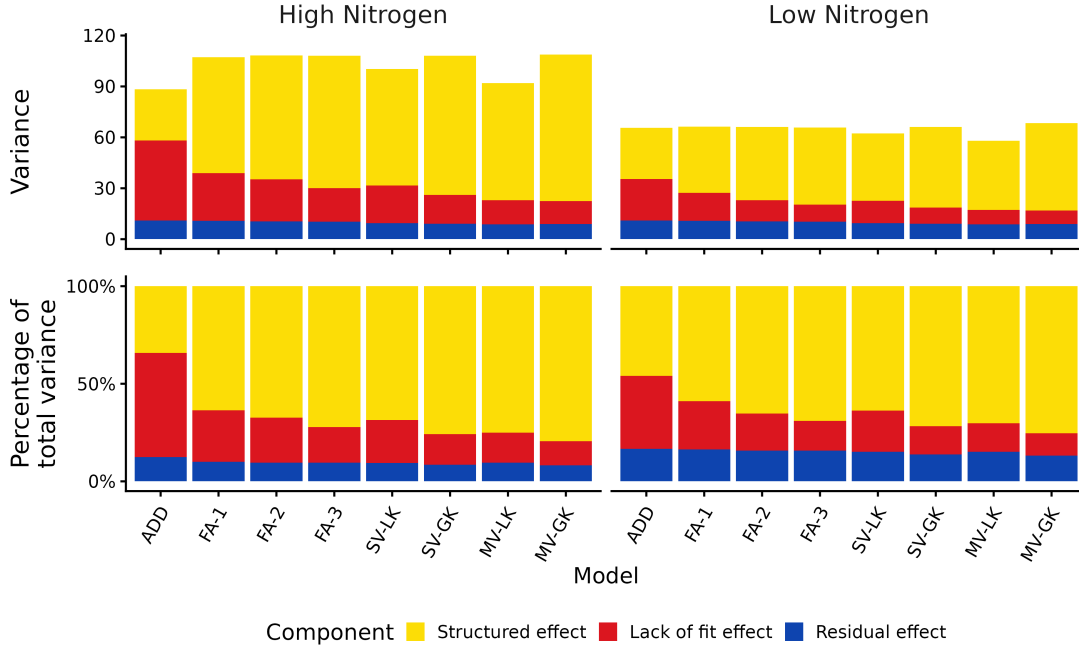


FIGURE 4. Partitioning of total variance of grain yield (overall means of 63.5 and 58.1 dt/ha for the high and low nitrogen managements, respectively) into variance captured by structured effects, lack of fit effects, and residual effects, averaged over the 13 environments and shown for each management of the BRI-WECS dataset. Note that the structured effect corresponds to the additive main effect for the ADD model, latent environmental covariables $\mathbf{\Lambda}\mathbf{\Lambda}^\top$ for the FA models, and kernel-based effects for the kernel models.

Next, we evaluated model performance in sparse testing genomic prediction scenarios with 8 levels of sparsity. Overall, the models incorporating $G \times E \times M$ interactions outperform the ADD model in terms of both correlation and RMSE (Figure 5). Furthermore, there is a clear trend for the $G \times E \times M$ models where performance increases as the level of sparsity decreases, with an improvement over the ADD model of about 8% at the least sparse end. The FA models of order 2 and 3 are most clearly affected by the lack of connectivity in the most sparse settings, where the performance drops to the level of the additive model in all cases except for the RMSE for the low nitrogen management. The kernel-based models generally perform reasonably well, although there is a large difference between the single and multiple variance versions. The multiple variance kernel models consistently outperform the single variance versions by a significant margin. The multiple variance Gaussian kernel model seems to slightly outperform the FA-1 model up to 25 checks, although differences are small. The higher order FA models clearly perform better after 25 checks, with the difference compared to the MV-GK model increasing as the level of sparsity decreases. Graphs showing genomic prediction accuracies for the different models and levels of sparsity for individual environments are provided in SM Figures S3–S6.

3.2. DROPS. The second dataset we use to illustrate the benchmark and kernel-based $G \times E \times M$ models is the DROPS dataset (Drought-tolerant yielding plants, Millet *et al.* 2019, 2016). It contains yield data on 246 maize hybrids in several locations across Europe and one in Chile in 2012 and 2013 under both irrigated and rain-fed watering regimes (Figure 3B). We computed the

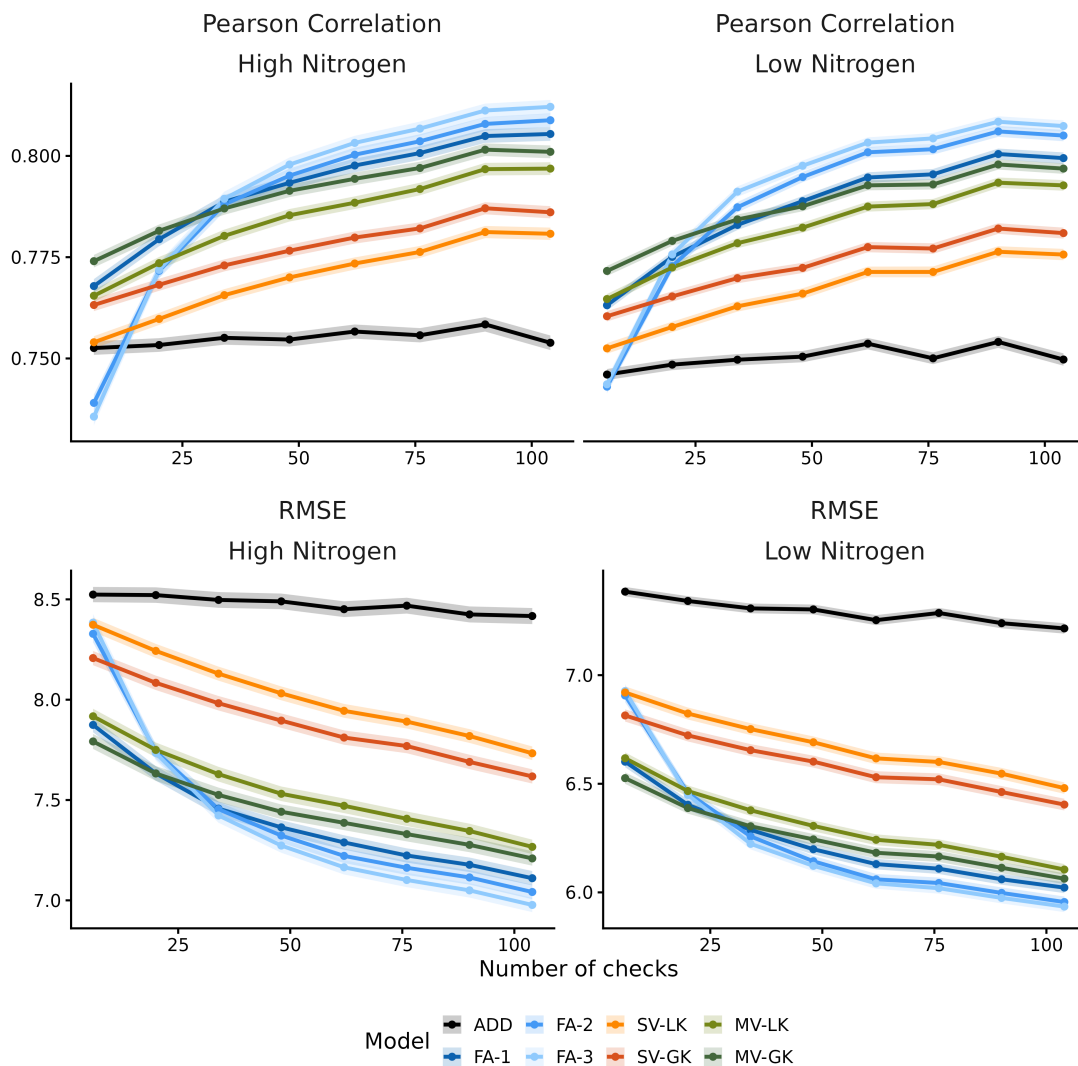


FIGURE 5. Pearson correlation and root mean squared error (RMSE) between BLUPs from the linear mixed models and centered test-set phenotypes for the BRIWECS dataset. Shaded areas represent standard errors. Accuracies are averaged over environments and shown separately for the low and high nitrogen managements. Checks are genotypes that are replicated in all environments. Note that as the number of checks increases, the sparsity in the sparse testing scenario decreases. Also note that the y-axes for RMSE have been scaled differently for clarity.

genomic relationship matrix using the 50K SNP markers available in the DROPS data repository and the `statgenGWAS` R-package, filtering any SNP markers with a minor allele frequency under 0.05 and using the identity by state method (van Rossum & Kruijer, 2025). The DROPS data repository at <https://doi.org/10.15454/IASSTN> contains pre-processed BLUEs for all $E \times M$ combinations. We thus performed no additional pre-processing and only subset these BLUEs to $E \times M$ combinations that had grain yield data on all 246 hybrids. We also discarded the Deb13

environment as it did not contain an irrigated trial. We randomly sampled 150 training and test sets for the sparse testing genomic prediction scenarios.

3.2.1. Pre-processing of environmental data and kernels. The DROPS data repository contains daily measurements from sowing to harvest on environmental covariables obtained from weather stations and other sensors. Like for the BRIWECS data, we first transformed the time-axis of these covariables from days to accumulated thermal time. We used equation (8), but changed the minimum (base) and maximum temperatures to 50 and 86 degrees Fahrenheit (North Dakota Agricultural Weather Network, 2025b). We used 12 of the environmental covariables to construct the kernels: RHmin.air, RHmax.air, RHmean.air, Raincum, Windspeedmax, ET0.air, Rad, Ri, VPD.air, VPD.apex, Tmax.apex, and Tnight. See the DROPS data repository for details on these covariables. We again scaled and centered the environmental covariables before computing the mean values for windows of 100 growing degree days and used these means as features to construct the kernels using (3) and (6).

3.2.2. Results. We fitted LMMs including an additional random effect with diagonal covariance structure as described in Section 2.3.1 to investigate the variance partitioning of the different models. Heritabilities for the DROPS dataset are significantly lower than for Briwecs at around 0.75 for the irrigated management and 0.64 for the rain-fed management. These heritabilities are in line with the estimates reported by Millet *et al.* (2016). Average total genetic variance, disregarding the ADD model, was larger for the irrigated management (0.865) than for the rain-fed management (0.502, Figure 6). The percentages of genetic variance explained by the covariables follow a similar trend to what was found in the Briwecs dataset. For the factor analytic models the percentages increase from 49% for the FA-1 model, to 60% for the FA-2 and 67% for the FA-3 model. Similarly, the explanatory power of the environmental covariables increases as the complexity of the kernels increases. While the differences between the linear kernels and Gaussian kernels are small at only 1 percentage point for both the single and multiple variance models, the impact of modeling multiple variances instead of a single variance is much larger. Percentages of genetic variance explained increased from 66% for the single variance models to 73% for the multiple variance models.

Finally, the percentage of genetic variance explained by the environmental covariables was larger for the rain-fed management than for the irrigated management. On average, approximately 71% of genetic variance was explained by the environmental covariables in the rain-fed management, compared to 68% for the irrigated management (Figure 6). This difference can likely be attributed to a decrease in the influence of the weather, modeled through the environmental covariables, due to active irrigation, showing that environmental covariables are more useful for modeling $G \times E$ in the absence of irrigation or other inputs. Interestingly, a similar result was found for the factor analytic models where on average the latent covariables explained 67% of genetic variance in the rain-fed management and only 54% in the irrigated management. For the benchmark ADD model the percentages of genetic variance explained by the main effect were again low at 49% for the rain-fed management and 32% for the irrigated management. Charts showing the variance partitioning for individual environments can be found in Figures S7 and S8 of the SM.

Results from the genomic prediction scenarios for the DROPS dataset are generally similar to those for the BRIWECS data. The ADD model performs worse than all interaction models, with the exception of the higher order FA models that show a significant drop in accuracy in the highly sparse scenarios (Figure 7). The Gaussian kernels outperform the linear kernels in terms of correlation as well as RMSE, with the multiple variance Gaussian kernel performing slightly better than the single variance version when considering RMSE. These results correspond to the proportions of genetic variance explained by the environmental covariables, and are likely again a result of the additional flexibility of the Gaussian kernels. In the most sparse settings, the Gaussian kernels perform better than the FA models. This remains true up to approximately

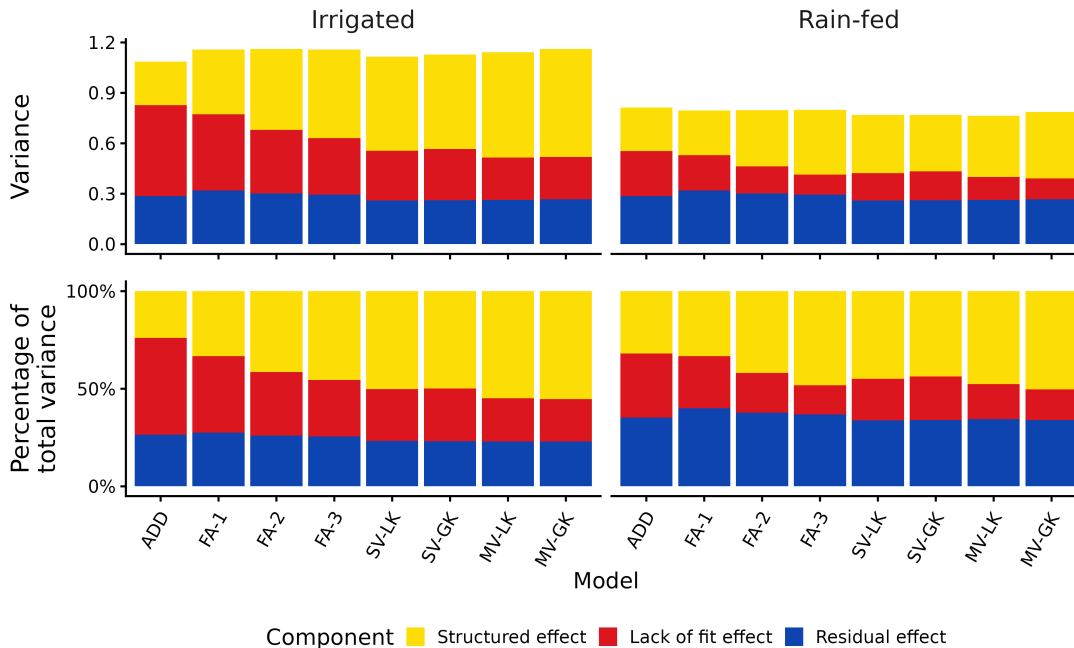


FIGURE 6. Partitioning of total variance of grain yield (overall means of 5.44 and 7.75 t/ha for the rain-fed and irrigated managements, respectively) into variance captured by structured effects, lack of fit effects, and residual effects, averaged over the 14 environments and shown for each management of the DROPS dataset. Note that the structured effect corresponds to the additive main effect for the ADD model, latent environmental covariables $\mathbf{\Lambda}\mathbf{\Lambda}^T$ for the FA models, and kernel-based effects for the kernel models.

40 checks, where the FA models start outperforming all other models. Interestingly, this also corresponds to the point where the higher-order FA models perform best, while only the FA-1 model remained somewhat competitive with the kernel models below 40 checks. Graphs showing genomic prediction accuracies for the different models and levels of sparsity for individual environments are provided in SM Figures S9–S12.

4. DISCUSSION

$G \times E \times M$ interactions are common in the breeding of field crops (de Leon *et al.*, 2016). Several models including these interactions in genomic predictions have been proposed, with REML estimation of structured covariance matrices and Bayesian implementations of kernel-based reaction norm models being two commonly used frameworks (Jarquín *et al.*, 2014; Gilmour *et al.*, 1995). Here, we made an effort to combine aspects from both frameworks by introducing REML implementations of several kernel based models with homo- and heterogeneous genetic variances for multi-environment, multi-management trial data. We have shown that a nonlinear Gaussian kernel combined with an unstructured model for managements and environment-specific variances increases the percentage of interaction variance explained by environmental covariables. We have also shown that these nonlinear kernel models improve $G \times E \times M$ predictions compared to factor analytic or linear kernel models in sparse testing scenarios.

Current implementations of kernel based models are limited in the sense that they only allow for a single genetic variance across all environments for any level of management. The benefit

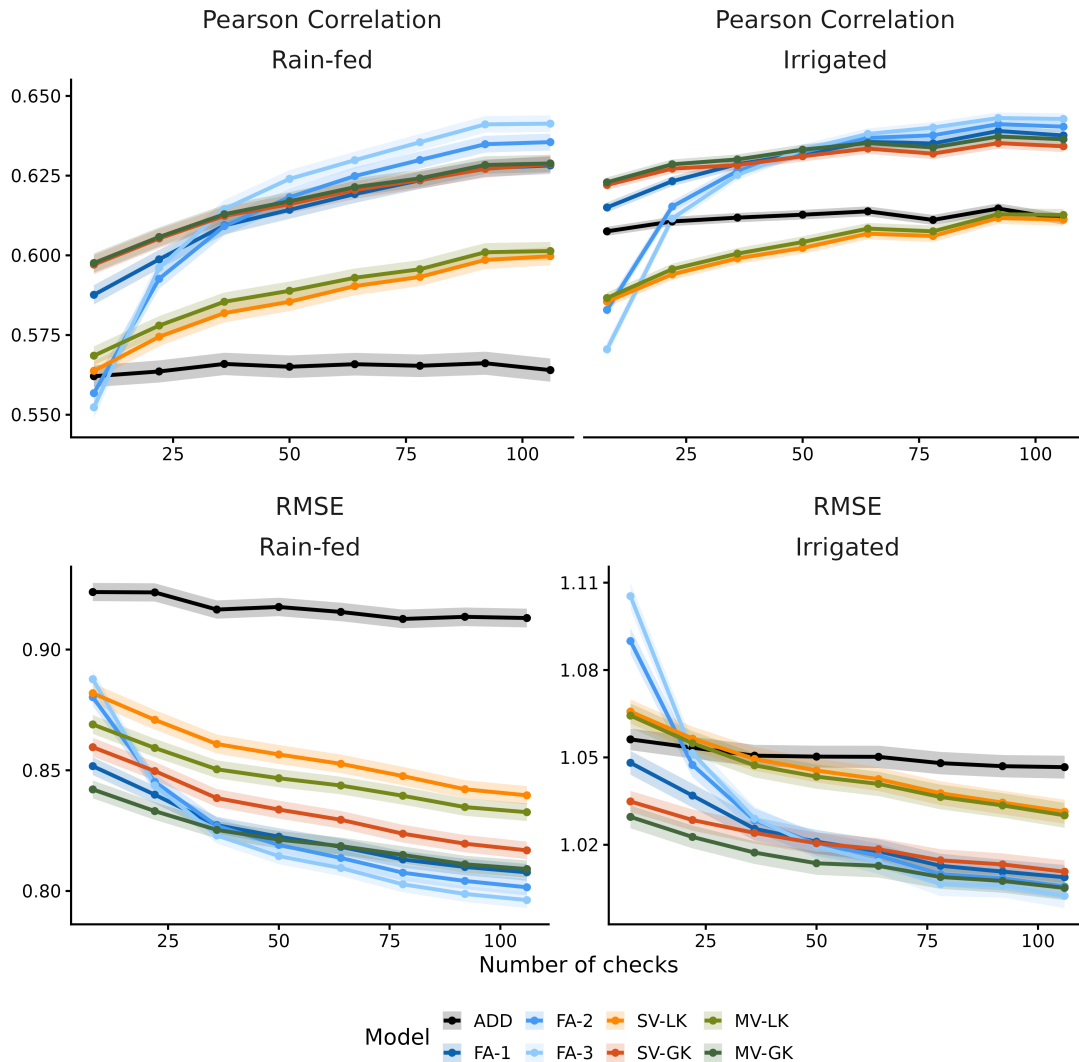


FIGURE 7. Pearson correlation and root mean squared error (RMSE) between BLUPs from the linear mixed models and centered test-set phenotypes for the DROPS dataset. Accuracies are averaged over environments and shown separately for the rain-fed and irrigated managements. Checks are genotypes that are replicated in all environments. Note that as the number of checks increases, the sparsity in the sparse testing scenario decreases. Also note that the y-axes for RMSE have been scaled differently for clarity.

of modeling environment-specific genetic variances can be easily explained from a shrinkage perspective. Homogeneous genetic variances for all environments for a given management results in equal shrinkage across all environments if the residual variances are assumed to be equal. Heterogeneity of genetic variance is well known to be a contributor to $G \times E$ interactions, and modeling environment-specific rates of shrinkage should improve predictive performance by reducing bias, as also shown by our results (Okeke *et al.*, 2017; van Eeuwijk *et al.*, 2016).

In addition to implementing kernel-based models with heterogeneous genetic variances, we provided a REML implementation of Gaussian kernel-based models where we treat the bandwidth of the kernel as a parameter to be estimated. There have been several approaches to choosing a bandwidth value. de Los Campos *et al.* (2010) proposed kernel averaging which involves modeling multiple random effects with different bandwidths. The variance components associated with these random effects then act as weights, resulting in an overall kernel that is essentially a weighed average of the kernels associated with each effect. A limitation of this approach is that the optimal bandwidth is approximated by summing multiple random effects, rather than estimated directly. The addition of these extra random effects increases the size of the mixed model equations, slowing down model fitting significantly. Other approaches typically involve cross-validation, some sort of grid-search, optimization before fitting the LMM, or are restricted to simple GBLUP models (Pérez-Elizalde *et al.*, 2015; Endelman, 2011). The REML estimation we proposed here extends this set of approaches and comes with the benefit that no cross-validation or optimization prior to fitting the model is required. Furthermore, our approach needs only one random effect as the bandwidth is estimated like any other parameter in the LMM in a single step. In fact, we can obtain any kernel $e^{-h\mathbf{D}}$ where $h \in (0, \infty)$ by simply treating the bandwidth as a strictly positive parameter. As a result, and depending on the data, we can obtain a diagonal covariance model $e^{-h\mathbf{D}} = \mathbf{I}_q$ as h approaches ∞ . Alternatively, we can obtain an additive main effects model $e^{-h\mathbf{D}} = \mathbf{J}_q$, where \mathbf{J}_q is an all-ones matrix of dimension $q \times q$, as h approaches 0. Finally, our implementation in standard software allows for easily combining the kernels with (un)structured covariance models for additional factors such as management as illustrated in this paper.

While our implementation allows for easily combining the environmental kernels with different covariance structures for factors such as managements, the structure imposed by the environmental kernels also allows for fitting additional random effects for the environment. Because of the structured and fixed nature of the linear kernels or distance matrices, the covariance models associated with these random effects can be unstructured. In the current paper, we fitted an additional random lack of fit effect for the environments with a diagonal covariance structure to investigate what proportion of $G \times E \times M$ variance was explained by the environmental covariables. The results revealed that total genetic variance was higher under the favorable management conditions, i.e., high nitrogen and irrigated trials, which matches what is commonly found in plant breeding experiments (Ud-Din *et al.*, 1992). More interestingly, the additional random effect revealed that the environmental covariables explained a larger percentage of the total $G \times E \times M$ variance under the rain-fed management practice with the MV-GK models explaining the largest percentage. These findings confirm the idea that modeling $G \times E$ using covariables obtained from weather stations is more useful for MET data obtained from trials with limited irrigation or other inputs. They also indicate that modeling $G \times E \times M$ data may not be as straightforward as fitting regression or reaction norm type models with what are essentially equal slopes for multiple managed treatments. Instead, modeling management-specific effects of environmental covariables, possibly using Gaussian kernels with management-specific bandwidths, may be more appropriate. This would somewhat relax the restrictions of the fully separable structure we currently used. While this may sound promising, we also want to stress the benefits of using a separable structure. By assuming that the covariance matrix of $E \times M$ combinations is a simple Kronecker product, and thus separable, we are able to obtain predictions for all $E \times M$ combinations even if environments and managements are heavily or fully confounded in the training data. This is especially useful when dealing with real-world datasets where typical management practices employed in trials vary with geographical location.

While in the current paper we only fitted an extra random effect with diagonal covariance matrix, the structure in the kernels allows for extensions with random effects with more complex covariance matrices as well. Our results with regards to variance partitioning show that both the kernel-based and FA models captured a significant part of the variance through their respective

structures based on (latent) covariables. If variance captured by the latent covariables is at least partly different from the variance captured by the observed covariables underlying the kernels, combining the FA and kernel structures would be an interesting way forward. In fact, combining the kernels with a random effect with factor analytic covariance structure would lead to a different parameterization of the integrated factor analytic linear mixed model (IFA-LMM) proposed by Tolhurst *et al.* (2022). Such models would offer a relatively straightforward implementation of what is essentially linear or nonlinear regression on known covariables, combined with linear regression on an additional set of latent environmental covariables.

Alternatively, the models discussed in this paper could be easily extended by including multiple kernels or kernels constructed using features retained after feature selection. Currently, we constructed environmental kernels using features representing all combinations of environmental covariables and days. We did not perform any feature selection, but it is well known that not all covariables and timeframes in the growth cycle are relevant (Millet *et al.*, 2019). Features representing different classes of covariables, e.g., temperature, radiation, or water availability could be used to construct different kernels. Variances associated with each kernel would then indicate the relevance of the different sets of features for predicting $G \times E$ (de Los Campos *et al.*, 2010). Similarly, kernels representing different growth stages could be included, or a kernel for environments could be combined with a non-linear kernel for genotypes instead of a kinship matrix.

Finally, it would be straightforward to adapt the $G \times E \times M$ models discussed in the current work to genotype by environment by trait ($G \times E \times T$) models for multi-trait genomic prediction. These models would allow for straightforward integration of secondary traits, possibly longitudinal and derived from high-throughput phenotyping (HTP), into $G \times E$ analyses. While modeling large numbers of HTP features directly is typically infeasible, a smaller number of features obtained after some form of dimension reduction can be modeled relatively easily. Many dimension reduction methods exist, but approaches that produce independent features such as factor or principal component analysis seem most promising due to the lower number of correlations that need to be estimated and the ability of these secondary features to improve predictions for a focal trait of interest (Melsen *et al.*, 2025).

5. CONCLUSION

This paper provides easy-to-use REML implementations of linear and nonlinear kernel-based genomic prediction models for $G \times E \times M$ data in standard mixed model software. We have shown that extending the basic kernel models that, given a particular management, assume a single genetic variance for all environments to models with environment-specific variances results in higher prediction accuracies. We have also shown that models with heterogeneous variances capture more of the $G \times E \times M$ interaction variance than the single variance versions, especially if combined with a nonlinear kernel. Finally, we have discussed some possible extensions to the different kernel-based models. Feature selection or kernels representing different subsets of environmental features deserve attention, as the inclusion of non-relevant features in kernels may lead to sub-optimal predictions. Furthermore, combining kernels with a factor analytic model leads to a straightforward implementation of the IFA-LMM model, separating the $G \times E$ in a component that can be predicted given environmental covariables and a component that cannot be predicted (Tolhurst *et al.*, 2022). Finally, we also recognize that the modeling of multiple traits or HTP features in a $G \times E$ context is easily implemented in the framework discussed in this paper by estimating correlations between traits instead of managements, offering a relatively straightforward way of integrating phenomics, enviromics, and genomics in a single LMM.

APPENDIX: PROGRAMMING FRAMEWORK AND PARTIAL DERIVATIVES

This Appendix contains a graphical overview and some information on the programming framework used to fit the kernel-based LMMs using the `own()` function of the `ASRem1-R` software. It also provides expressions for the partial derivatives of the different kernel-based covariance models required to fit them using `ASRem1-R`.

Programming framework. We make use of the `own()` function available in the R-package `asrem1` (`ASRem1-R` version 4.2) to fit the kernel-based LMMs. The `own()` function allows specification of custom covariance models associated with random effects in the LMM through an external variance function. It thus allows us to model the management and environment factors using either a single variance for each level of management, resulting in the same variance for all combinations of environments and that specific management, or unique variances for all environment-management combinations. Furthermore, it allows us to model Gaussian kernels for which the bandwidth parameters are estimated directly using REML.

The use of `own()` is illustrated in Figure 8. Within the `asrem1()` call, `own()` is used to specify the random part of the model, taking five arguments. The argument `obj` specifies which factor in the data passed to `asrem1()` should be modeled using the custom covariance structure, similarly to how the factor is specified for functions like `corgh()`, `fa()`, or `vm()`. The `fun` argument takes a character variable referring to the name of the user-defined external variance function, e.g., `"varFun"`. Finally, the `init`, `type`, and `con` arguments take vectors that allow specification of the initial values, types, and constraints for the parameters used to construct the custom covariance matrix. We refer to the `ASRem1-R` Reference Manual Version 4.2 by Butler *et al.* (2023) for more information.

The external variance function itself must be defined in the R environment prior to calling `asrem1()`. It must have the arguments `order` and `kappa`, and no others. While fitting the LMM, `asrem1()` calls `own()` at every iteration, passing the number of levels of the factor specified using `obj` as `order` and current parameter estimates as `kappa`. Note that for the first iteration, `kappa` will hold the initial values specified using `init`. Inside the external variance function, `order` and `kappa` are then used to construct the covariance matrix and partial derivative matrices with respect to all parameters. These are then returned as a list of matrices with the covariance matrix coming first, followed by all derivatives with respect to the parameters in the same order as `kappa`. In other words, if the first element of `kappa` is the first variance, the second element in the returned list must be the derivative of the covariance matrix with respect to the first variance.

The `asrem1()` function then uses the returned covariance matrix and derivatives to update the parameter estimates, before calling `own()` again. The cycle illustrated in Figure 8 continues in this way until convergence or the maximum number of iterations is reached. The `own()` function provides a powerful interface to `ASRem1-R`, allowing specification of any valid covariance structure for which derivatives can be obtained. We provide expressions for the partial derivative matrices of the kernel-based covariance models in the remainder of this Appendix.

Partial derivatives. This Section provides expressions for the partial derivatives of the different kernel-based covariance models with respect to the parameters used for the management and environment factors. Note that the kinship matrix \mathbf{K}_G has been left out as it is a constant and the same for all models.

Single variance linear kernel. The parameters for the single variance linear kernel (SV-LK) model consist of p genetic variances and $up/2$ genetic correlations where $u = p - 1$:

$$\boldsymbol{\kappa} = [\sigma_1^2, \sigma_2^2, \dots, \sigma_p^2, \rho_{12}, \rho_{13}, \dots, \rho_{up}],$$

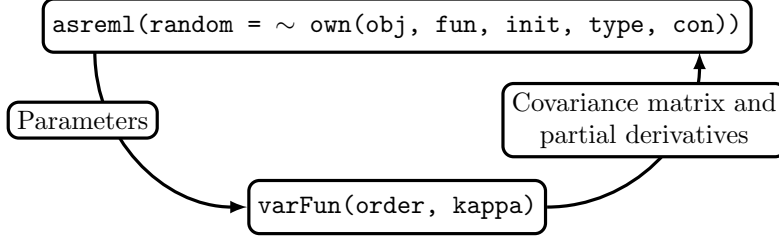


FIGURE 8. Programming framework for specifying custom covariance models in **ASReml-R**. The `own()` function can be used inside the `asreml()` call. Arguments `obj`, `fun`, `init`, `type`, and `con` are used to specify the data factor, name of the custom external variance function, initial values for the (variance) parameters, types of parameters, and parameter constraints. The custom variance function itself must only have arguments `order` and `kappa` which take the number of factor levels and parameter estimates at a particular iteration, respectively, as passed by **ASReml-R** during model fitting.

resulting in the following derivatives with respect to the variances:

$$(9) \quad \frac{\partial(\boldsymbol{\Sigma}_M \otimes \mathbf{K}_E)}{\partial \sigma_i^2} = \frac{\boldsymbol{\Sigma}_M \circ (\mathbf{A}_i + \mathbf{A}_i^\top)}{\sigma_i^2} \otimes \mathbf{K}_E,$$

where \mathbf{A}_i is a $p \times p$ matrix containing 0.5 in the i th row, and zero everywhere else. The SV-LK model produces the following derivatives with respect to the correlations:

$$(10) \quad \frac{\partial(\boldsymbol{\Sigma}_M \otimes \mathbf{K}_E)}{\partial \rho_{ii'}} = (\mathbf{s}_M \mathbf{s}_M^\top \circ \mathbf{B}_{ii'}) \otimes \mathbf{K}_E,$$

where $\mathbf{B}_{ii'} \in \mathbb{R}^{p \times p}$ is an indicator matrix where $\mathbf{B}_{ii'} = \mathbf{B}_{i'i} = 1$ and all other elements are zero. The vector \mathbf{s}_M contains standard deviations for each level of management so that $\mathbf{s}_M \mathbf{s}_M^\top \circ \mathbf{R}_M = \boldsymbol{\Sigma}_M$.

Multiple variance linear kernel. The multiple variance linear kernel (MV-LK) model extends the previous model by allowing for heterogeneous genetic variances, providing environment-specific rates of shrinkage for a given management. The number of parameters thus increases to pq variances for all $E \times M$ combinations and $up/2$ correlations between the different managements:

$$\boldsymbol{\kappa} = [\sigma_1^2, \sigma_2^2, \dots, \sigma_{pq}^2, \rho_{12}, \rho_{13}, \dots, \rho_{up}].$$

The partial derivatives with respect to the variances are given by

$$(11) \quad \frac{\partial[\mathbf{ss}^\top \circ (\mathbf{R}_M \otimes \mathbf{K}_E)]}{\partial \sigma_l^2} = \frac{\mathbf{ss}^\top \circ (\mathbf{R}_M \otimes \mathbf{K}_E)}{\sigma_l^2} \circ (\mathbf{A}_l + \mathbf{A}_l^\top),$$

where $\mathbf{A}_l \in \mathbb{R}^{pq \times pq}$ now contains 0.5 in the row corresponding to $E \times M$ combination l . The derivatives with respect to the correlations can be obtained by

$$(12) \quad \frac{\partial[\mathbf{ss}^\top \circ (\mathbf{R}_M \otimes \mathbf{K}_E)]}{\partial \rho_{ii'}} = \mathbf{ss}^\top \circ (\mathbf{B}_{ii'} \otimes \mathbf{K}_E).$$

Single variance Gaussian kernel. The parameters and derivatives for the SV-GK model are identical to those given in (9) and (10), except for the fact that \mathbf{K}_E is replaced by $e^{-h\mathbf{D}_E}$ and there is the additional parameter h for which the derivative is

$$\frac{\partial(\boldsymbol{\Sigma}_M \otimes e^{-h\mathbf{D}_E})}{\partial h} = \boldsymbol{\Sigma}_M \otimes (-\mathbf{D}_E \circ e^{-h\mathbf{D}_E}).$$

Multiple variance Gaussian kernel. Similarly, the derivatives with respect to the variances and correlations for the MV-GK model can be obtained by replacing \mathbf{K}_E by $e^{-h\mathbf{D}_E}$ in (11) and (12). The derivative with respect to the bandwidth is then

$$\frac{\partial \left[\mathbf{ss}^\top \circ (\mathbf{R}_M \otimes e^{-h\mathbf{D}_E}) \right]}{\partial h} = \mathbf{ss}^\top \circ \left[\mathbf{R}_M \otimes (-\mathbf{D}_E \circ e^{-h\mathbf{D}_E}) \right].$$

REFERENCES

- Bančić, J., Gorjanc, G. & Tollhurst, D.J. (2024). A framework for simulating genotype-by-environment interaction using multiplicative models. *Theoretical and Applied Genetics* **137**, 197. <https://doi.org/10.1007/s00122-024-04644-7>
- Bandeira e Sousa, M., Cuevas, J., de Oliveira Couto, E.G., Pérez-Rodríguez, P., Jarquín, D., Fritsche-Neto, R., Burgueño, J. & Crossa, J. (2017). Genomic-enabled prediction in Maize using kernel models with genotype \times environment interaction. *G3* **7**, 1995–2014. <https://doi.org/10.1007/s00122-024-04644-7>
- Bernardo, R. (1994). Prediction of Maize single-cross performance using RFLPs and information from related hybrids. *Crop Science* **34**, 20–25. <https://doi.org/10.2135/cropsci1994.0011183X003400010003x>
- Boer, M.P. (2023). Tensor product p-splines using a sparse mixed model formulation. *Statistical Modelling* **23**, 465–479. <https://doi.org/10.1177/1471082X231178591>
- Butler, D.G., Cullis, B.R., Gilmour, A.R., Gogel, B.G. & Thompson, R. (2023). ASReml-R Reference Manual Version 4.2. *VSN International Ltd., Hemel Hempstead, England* <https://doi.org/10.1534/genetics.114.164442>
- Cooper, M., Messina, C.D., Tang, T., Gho, C., Powell, O.M., Podlich, D.W., Technow, F., & Hammer, G.L. (2022). Predicting genotype \times environment \times management (G \times E \times M) interactions for the design of crop improvement strategies. In *Plant Breeding Reviews*, I. Goldman. (Ed.). <https://doi.org/10.1002/9781119874157.ch8>
- Cooper, M., Chapman, S.C., Podlich, D.W., & Hammer, G.L. (2002). The GP problem: Quantifying gene-to-phenotype relationships. *In Silico Biology* **2**, 151–164. <https://doi.org/10.3233/ISB-00032>
- Costa-Neto, G., Fritsche-Neto, R. & Crossa, J. (2021a). Nonlinear kernels, dominance, and envirotyping data increase the accuracy of genome-based prediction in multi-environment trials. *Heredity* **126**, 92–106. <https://doi.org/10.1038/s41437-020-00353-1>
- Costa-Neto, G., Galli, G., Carvalho, H.F., Crossa, J. & Fritsche-Neto, R. (2021b). EnvRtype: a software to interplay enviromics and quantitative genomics in agriculture. *G3* **11**, jkab040. <https://doi.org/10.1093/g3journal/jkab040>
- Crossa, J., Fritsche-Neto, R., Montesinos-Lopez, O.A., Costa-Neto, G., Dreisigacker, S., Montesinos-Lopez, A. & Bentley, A.R. (2021). The modern plant breeding triangle: Optimizing the use of genomics, phenomics, and enviromics data. *Frontiers in Plant Science* **12**, 651480. <https://doi.org/10.3389/fpls.2021.651480>
- Crossa, J., Pérez-Rodríguez, P., Cuevas, J., Montesinos-López, O., Diego Jarquín, D., de los Campos, G., Burgueño, G., González-Camacho, J.M., Pérez-Elizalde, S., Beyene, Y., Dreisigacker, S., Singh, R. Zhang, X., Gowda, M., Roorkiwal, M., Rutkoski, J. & Varshney, R.K. (2017). Genomic selection in plant breeding: Methods, models, and perspectives. *Trends in Plant Science* **22**, 961–975. <https://doi.org/10.1016/j.tplants.2017.08.011>
- de Leon, N., Jannink, J.L., Edwards, J.W. & Kaeppler, S.M. (2016). Introduction to a special issue on genotype by environment interaction. *Crop Science* **56**, 2081–2089. <https://doi.org/10.2135/cropsci2016.07.0002in>
- de los Campos, G., Gianola, D., Rosa, G.J.M., Weigel, K.A. & Crossa, J. (2010). Semi-parametric genomic-enabled prediction of genetic values using reproducing kernel Hilbert spaces methods. *Genetics Research* **92**, 295–308. <https://doi.org/10.1017/S0016672310000285>

- Eberhart, M. (1970). Factors affecting efficiencies of breeding methods. *African Soils* **15**, 655–680.
- Endelman, J.B. (2011). Ridge regression and other kernels for genomic selecting with R package rrBLUP. *The Plant Genome* **4**, 250–255. <https://doi.org/10.3835/plantgenome2011.08.0024>
- Falconer, D.S. & Mackay, T.F.C. (1996). Introduction to quantitative genetics, 4th edition. *Addison Wesley Longman, Harlow, England*.
- Gezan, S., de Oliveira, A.A., Galli, G., & Murray, D. (2022). ASRgenomics: An R package with complementary genomic functions. *VSN International, Hemel Hempstead, United Kingdom*
- Gogna, A., Schulthess, A.W., Röder, M.S., Ganal, M.W. & Reif, J.C. (2022). Gabi wheat a panel of European elite lines as central stock for wheat genetic research. *Scientific Data* **9**, 538. <https://doi.org/10.1038/s41597-022-01651-5>
- Gilmour, A.R., Thompson, R. & Cullis, B.R. (1995). Average information REML: An efficient algorithm for variance parameter estimation in linear mixed models. *Biometrics* **51**, 1440–1450. <https://doi.org/10.2307/2533274>
- Jarquín, D., Crossa, J., Lacaze, X., Cheyron, P.D., Daucourt, J., Lorgeou, J., Piraux, F., Guerreiro, L., Pérez, P., Calus, M., Burgueño, J. & de los Campos, G. (2014). A reaction norm model for genomic selection using high-dimensional genomic and environmental data. *Theoretical and Applied Genetics* **127**, 595–607. <https://doi.org/10.1007/s00122-013-2243-1>
- Jarquín, D., Howard, R., Crossa, J., Beyene, Y., Gowda, M., Martini, J.W.R., Pazaran, G.C., Burgueño, J., Pacheco, A., Grondona, M., Wimmer, V. & Prasanna, B.M. (2020). Genomic prediction enhanced sparse testing for multi-environment trials. *G3* **10**, 2725–2739. <https://doi.org/10.1534/g3.120.401349>
- Keerthi, S.S. & Lin, C. (2003). Asymptotic behaviors of support vector machines with Gaussian kernel. *Neural Computation* **15**, 1667–1689. <https://doi.org/10.1162/089976603321891855>
- Li, Z. & Sillanpää, M.J. (2012). Overview of LASSO-related penalized regression methods for quantitative trait mapping and genomic selection. *Theoretical and Applied Genetics* **125**, 419–435. <https://doi.org/10.1007/s00122-012-1892-9>
- Lichthardt, C., Chen, T.W., Stahl, A. & Stützel, H. (2019). Co-evolution of sink and source in the recent breeding history of winter wheat in Germany. *Frontiers in Plant Science* **10**, 1771. <https://doi.org/10.3389/fpls.2019.01771>
- Malosetti, M., Voltas, J., Romagosa, I., Ullrich, S.E. & van Eeuwijk, F.A. (2004). Mixed models including environmental covariables for studying QTL by environment interaction. *Euphytica* **137**, 139–145. <https://doi.org/10.1023/B:EUPH.0000040511.46388.ef>
- Malosetti, M., Ribaut, J. & van Eeuwijk, F.A. (2013). The statistical analysis of multi-environment data: modeling genotype-by-environment interaction and its genetic basis. *Frontiers in Physiology* **4**, 44. <https://doi.org/10.3389/fphys.2013.00044>
- Martini, J.W.R., Crossa, J., Toledo, F.H. & Cuevas, J. (2020). On Hadamard and Kronecker products in covariance structures for genotype \times environment interaction. *The Plant Genome* **13**, e20033. <https://doi.org/10.1002/tpg2.20033>
- Melsen, K.A.C., Kunst, J.F., Crossa, J., Krause, M.R., van Eeuwijk, F.A., Kruijer, W. & Peeters, C.F.W. (2025). Improving genomic prediction using high-dimensional secondary phenotypes: The genetic latent factor approach. *Biometrical Journal* **67**, e70081. <https://doi.org/10.1002/bimj.70081>
- Meuwissen, T.H., Hayes, B.J. & Goddard, M.E. (2001). Prediction of total genetic value using genome-wide dense marker maps. *Genetics* **157**, 1819–1829. <https://doi.org/10.1093/genetics/157.4.1819>
- Millet, E.J., Kruijer, W., Coupel-Ledru, A., Prado, S.A., Cabrera-Bosquet, L., Lacube, S., Charcosset, A., Welcker, C., van Eeuwijk, F. & Tardieu, F. (2019). Genomic prediction of maize yields across European environmental conditions. *Nature Genetics* **51**, 952–956. <https://doi.org/10.1038/s41588-019-0488-8>

- [//doi.org/10.1038/s41588-019-0414-y](https://doi.org/10.1038/s41588-019-0414-y)
- Millet, E.J., Welcker, C., Kruijer, W., Negro, S., Coupel-Ledru, A., Nicolas, S.D., Laborde, J., Bauland, C., Praud, S., Ranc, N., Presterl, T., Tuberosa, R., Bedo, Z., Draye, X., Usadel, B., Charcosset, A., van Eeuwijk, F. & Tardieu, F. (2016). Genome-wide analyses of yield in Europe: Allelic effects vary with drought and heat scenarios. *Plant Physiology* **172**, 749–764. <https://doi.org/10.1104/pp.16.00621>
- Monteiro, L.A., Sentelhas, P.C. & Pedra, G.U. (2017). Assessment of NASA/POWER satellite-based weather system for Brazilian conditions and its impact on sugarcane yield simulation. *International Journal of Climatology* **38**, 1571–1581. <https://doi.org/10.1002/joc.5282>
- Montesinos-López, O.A., Montesinos-López, A. & Crossa, J. (2022). Multivariate statistical machine learning methods for genomic prediction. *Springer Cham, Switzerland*. <https://doi.org/10.1038/s41437-021-00412-1>
- Montesinos-López, A., Montesinos-López, O.A., Montesinos-López, J.C., Flores-Cortés, C.A., de la Rosa, R. & Crossa, J. (2021). A guide for kernel generalized regression methods for genomic-enabled prediction. *Heredity* **126**, 577–596. <https://doi.org/10.1038/s41437-021-00412-1>
- North Dakota Agricultural Weather Network (2025a). Wheat growth stage prediction using growing degree days (GDD). <https://ndawn.ndsu.nodak.edu/help-wheat-growing-degree-days.html>
- North Dakota Agricultural Weather Network (2025b). Corn growing degree Days (GDD). <https://ndawn.ndsu.nodak.edu/help-corn-growing-degree-days.html>
- Okeke, U.G., Akdemir, D., Rabbi, I., Kulakow, P. & Jannink, J. (2017). Accuracies of univariate and multivariate genomic prediction models in African cassava. *Genetics Selection Evolution* **49**, 88. <https://doi.org/10.1186/s12711-017-0361-y>
- Pérez-Elizalde, S., Cuevas, J., Pérez-Rodríguez, P. & Crossa, J. (2015). Selection of the bandwidth parameter in a Bayesian kernel regression model for genomic-enabled prediction. *Journal of Agricultural, Biological, and Environmental Statistics* **20**, 512–532. <https://doi.org/10.1007/s13253-015-0229-y>
- Pérez-Enciso, M. & Zingaretti, L.M. (2019). A guide on deep learning for complex trait genomic prediction. *Genes* **10**, 553. <https://doi.org/10.3390/genes10070553>
- Pérez-Rodríguez, P. & de los Campos, G. (2022). Multitrait Bayesian shrinkage and variable selection models with the BGLR-R package. *Genetics* **222**, iyac112. <https://doi.org/10.1093/genetics/iyac112>
- Piepho, H. & Williams, E. (2024). Factor-analytic variance-covariance structures for prediction into a target population of environments. *Biometrical Journal* **66**, e202400008. <https://doi.org/10.1002/bimj.202400008>
- Ring, M. & Eskofier, B.M. (2016). An approximation of the Gaussian RBF kernel for efficient classification with SVMs. *Pattern Recognition Letters* **84**, 107–113. <https://doi.org/10.1016/j.patrec.2016.08.013>
- Rodríguez-Álvarez, M.X., Boer, M.P., van Eeuwijk, F.A. & Eilers, P.H.C. (2018). Correcting for spatial heterogeneity in plant breeding experiments with p-splines. *Spacial Statistics* **23**, 52–71. <https://doi.org/10.1016/j.spasta.2017.10.003>
- Runcie, D. & Cheng, H. (2019). Pitfalls and remedies for cross validation with multi-trait genomic prediction methods. *G3* **9**, 3727–33741. <https://doi.org/10.1534/g3.119.400598>
- Schölkopf, B. (2000). The kernel trick for distances. In Leen, T., Dietterich, T. & Tresp, V. (Eds), *Advances in Neural Information Processing Systems 13*.
- Tolhurst, D.J., Gaynor, R.C., Gardunia, B., Hickey, J.M. & Gorjanc, G. (2022). Genomic selection using random regressions on known and latent environmental covariates. *Theoretical and Applied Genetics* **135**, 3393–3415. <https://doi.org/10.1007/s00122-022-04186-w>
- Tolhurst, D.J., Mathews, K.L., Smith, A.B. & Cullis, B.R. (2019). Genomic selection in multi-environment plant breeding trials using a factor analytic linear mixed model. *Journal of Animal Breeding and Genetics* **136**, 279–300. <https://doi.org/10.1111/jbg.12404>

- Ud-Din, N., Carver, B.F. & Clutter, A.C. (1992). Genetic analysis and selection for wheat yield in drought-stressed and irrigated environments. *Euphytica* **62**, 89–96. <https://doi.org/10.1007/BF00037933>
- VanRaden, P.M. (2008). Efficient methods to compute genomic predictions. *Journal of Dairy Science* **91**, 4414–4423. <https://doi.org/10.3168/jds.2007-0980>
- van Eeuwijk, F.A., Bustos-Korts, D.V. & Malosetti, M. (2016). What should students in plant breeding know about the statistical aspects of genotype x environment interactions? *Crop Science* **56**, 2119–2140. <https://doi.org/10.2135/cropsci2015.06.0375>
- van Rossum, B. & Kruijer, W. (2025). statgenGWAS: Genome wide association studies. *R package version 1.0.12*. <https://biometris.github.io/statgenGWAS/index.html>
- Vert, J.P., Tsuda, K. & Schölkopf, B. (2004). A primer on kernel methods. In Schölkopf, B., Tsuda, K. & Vert J.P. (Eds), *The MIT Press, Cambridge, MA, United States*.
- Wang, T.C., Rose, T., Zetzsche, H., Ballvora, A., Friedt, W., Kage, H., Léon, J., Lichthardt, C., Ordon, F., Snowdon, R.J., Stahl, A., Stützel, H., Wittkop, B. & Chen, T.W. (2025). Multi-environment field trials for wheat yield, stability and breeding progress in Germany. *Scientific Data* **12**, 64. <https://doi.org/10.1038/s41597-024-04332-7>

Supplementary Material: REML implementations of kernel-based genomic prediction models for genotype \times environment \times management interactions

Killian A.C. Melsen^{1*}, Salvador Gezan², Daniel J. Tolhurst³, Fred A. van Eeuwijk¹, Carel F.W. Peeters¹

¹Mathematical & Statistical Methods group - Biometris, Wageningen University & Research, PO Box 16, 6700 AA, Wageningen, The Netherlands

²VSN International, 2 Amberside House, Wood Lane, HP2 4TP, Hemel Hempstead, United Kingdom

³The Roslin Institute and Royal (Dick) School of Veterinary Science, University of Edinburgh, Easter Bush, Midlothian, EH25 9RG, United Kingdom

* killian.melsen@wur.nl

TABLE S1. Overview of the geographical coordinates, sowing, and harvest dates (yyyy-mm-dd) to obtain environmental covariables for the 14 environments in the BRIWECS dataset. The environmental covariables used for the kernels included RH2M, WS2M, PRECTOT, EVPTRNS, P_ETP, VPD, ALLSKY_SFC_LW_DWN, ALLSKY_SFC_SW_DWN, ALLSKY_SFC_SW_DNI, ALLSKY_SFC_PAR_TOT, ALLSKY_SFC_UVA, ALLSKY_SFC_UVB, RTA, n, N, T2M, T2M.MAX, and T2M.MIN. See the documentation of the `EnvRtype::get_weather()` function for details on these covariables.

Environment	Latitude	Longitude	Sowing date	Harvest date
HAN_2015	52.24382	9.818108	2014-10-28	2015-07-22
HAN_2016	52.24382	9.818108	2015-11-04	2016-07-10
HAN_2017	52.24382	9.818108	2016-11-01	2017-07-09
KAL_2015	50.61310	6.994236	2014-10-28	2015-07-13
KAL_2016	50.61310	6.994236	2015-10-28	2016-07-21
KAL_2017	50.61310	6.994236	2016-10-26	2017-07-08
KIE_2015	54.31568	9.980414	2014-10-23	2015-07-13
KIE_2016	54.31568	9.980414	2015-10-02	2016-06-21
KIE_2017	54.31568	9.980414	2016-09-21	2017-07-22
QLB_2015	51.76921	11.145669	2014-10-18	2015-07-07
QLB_2016	51.76921	11.145669	2015-10-10	2016-07-07
QLB_2017	51.76921	11.145669	2016-11-02	2017-07-10
RHH_2015	50.76050	8.875599	2014-10-28	2015-07-18
RHH_2016	50.76050	8.875599	2015-10-20	2016-07-09

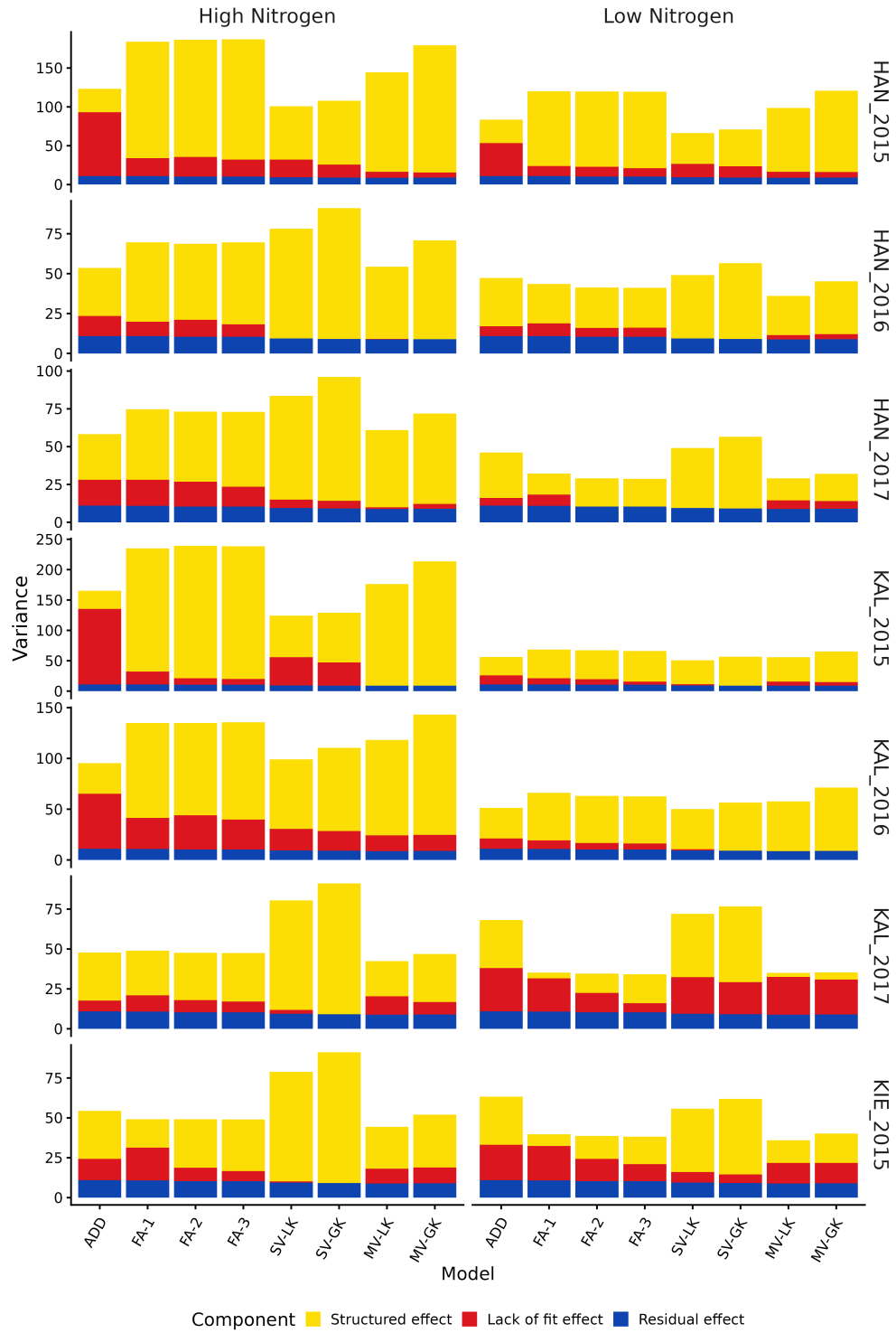


FIGURE S1. Partitioning of $G \times E \times M$ variance into structured, lack of fit, and residual effects for each environment in the BRIWECS dataset.

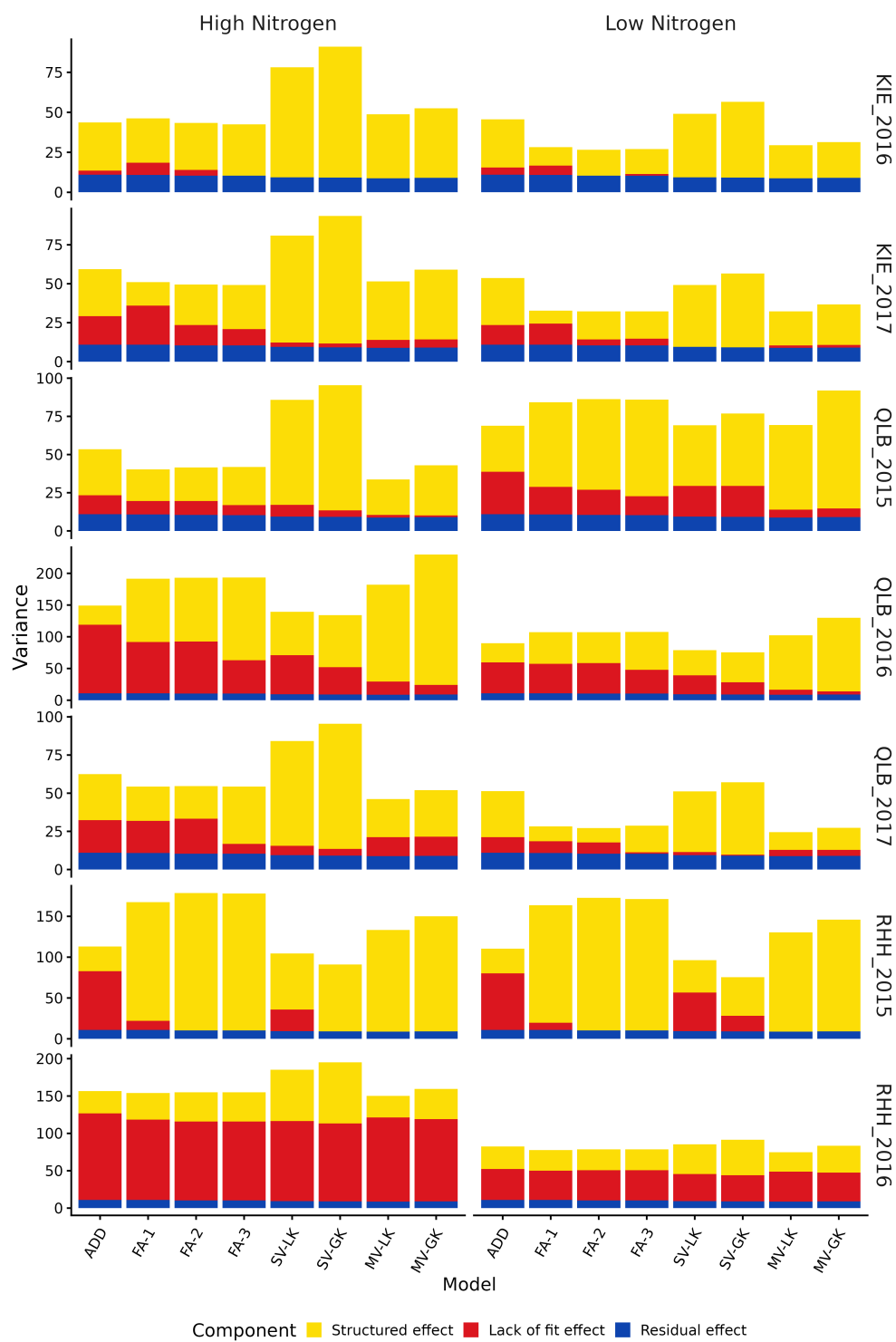


FIGURE S2. Continued. Partitioning of $G \times E \times M$ variance into structured, lack of fit, and residual effects for each environment in the BRIWECS dataset.

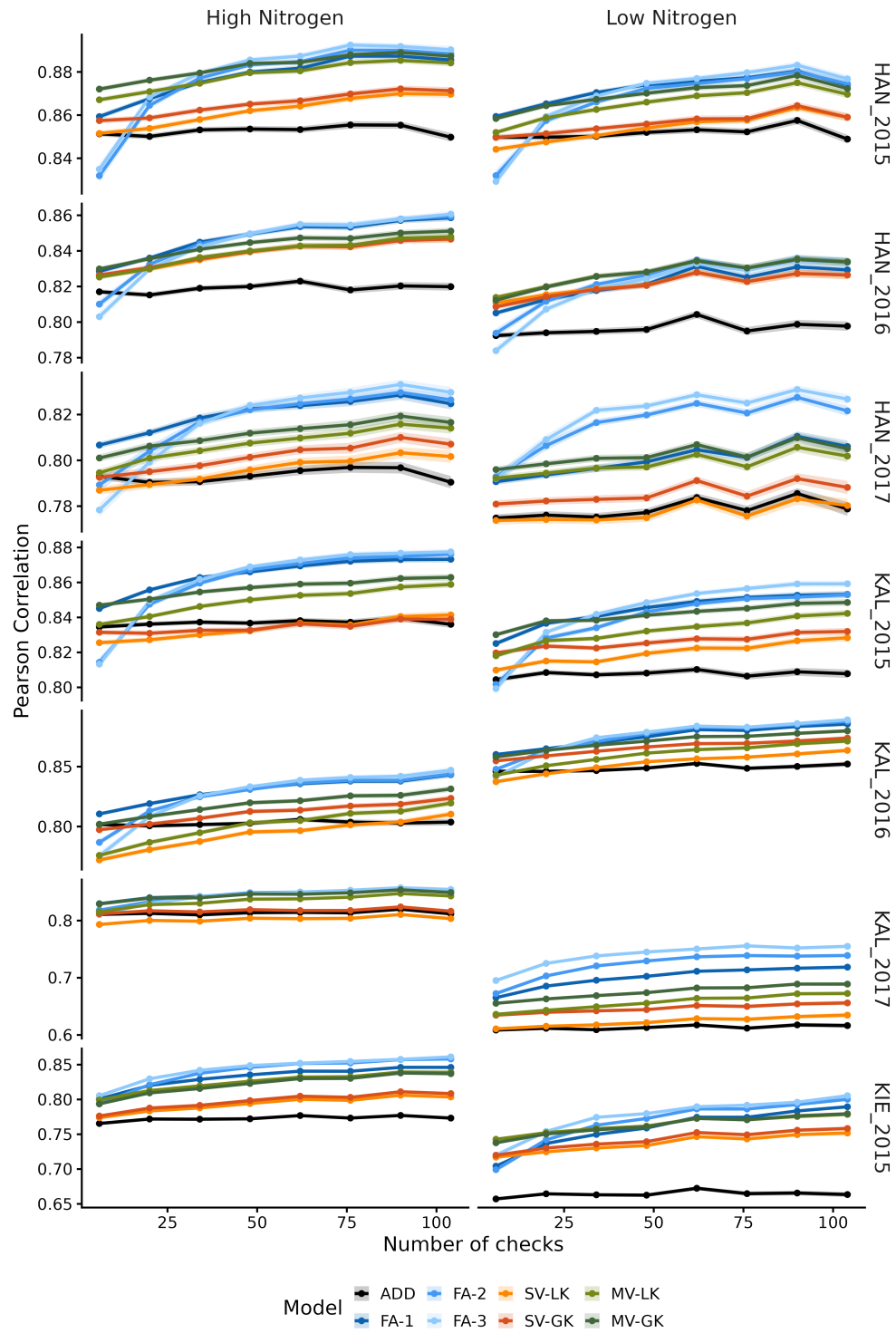


FIGURE S3. Pearson correlation between BLUPs from the LMMs and centered test-set phenotypes for the BRIWECS dataset for each environment. Shaded areas represent standard errors.

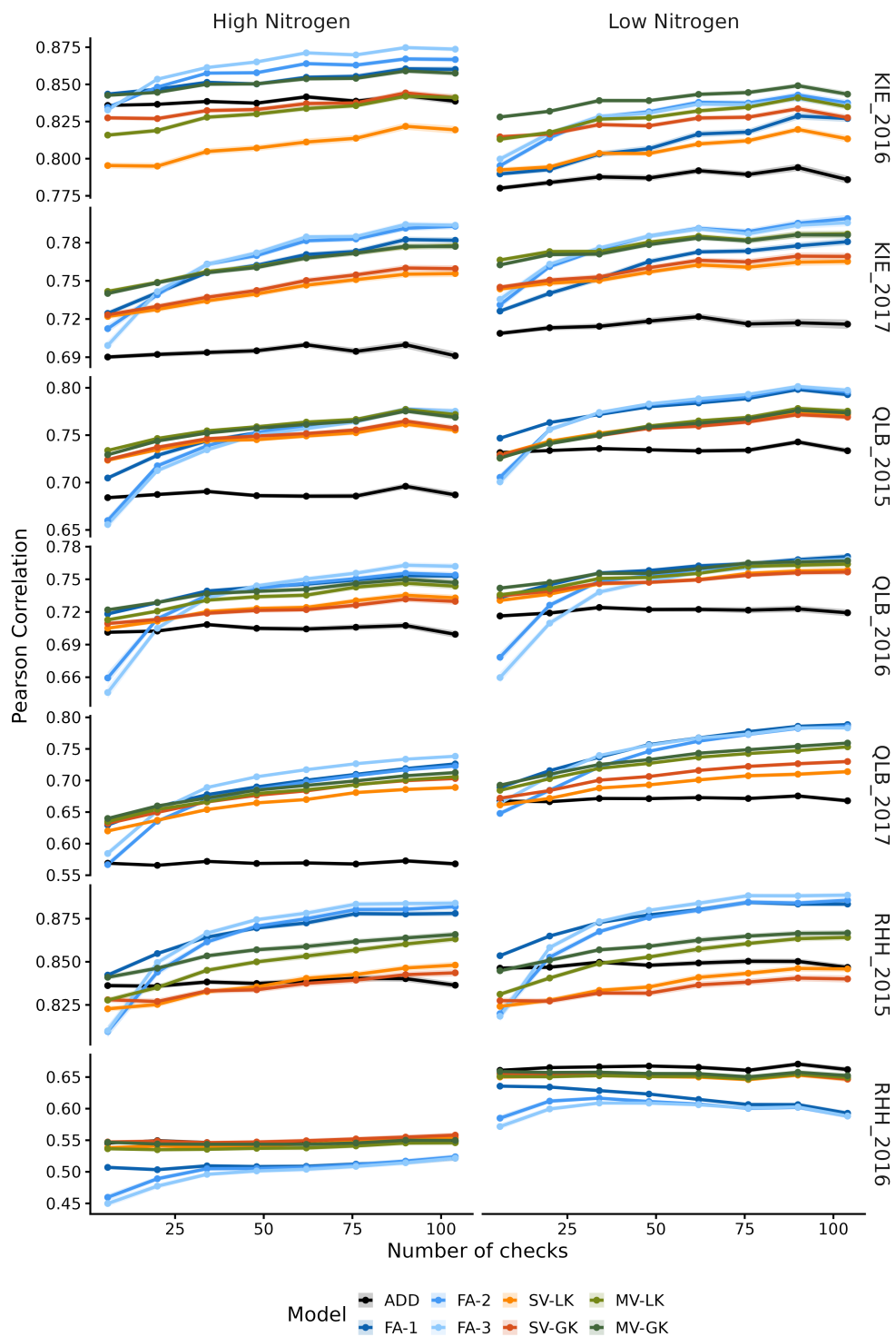


FIGURE S4. Continued. Pearson correlation between BLUPs from the LMMs and centered test-set phenotypes for the BRIWECS dataset for each environment. Shaded areas represent standard errors.

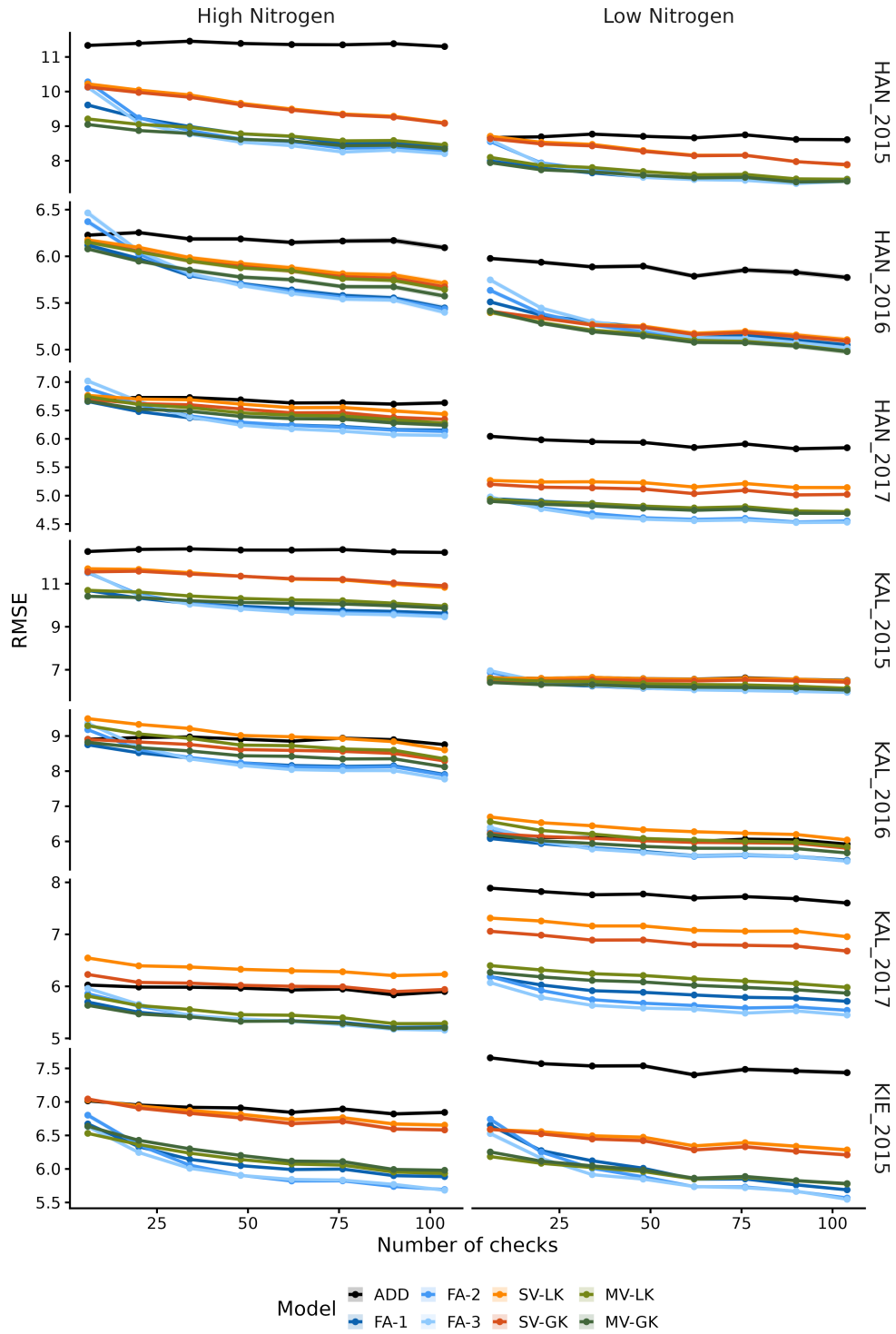


FIGURE S5. RMSE between BLUPs from the LMMs and centered test-set phenotypes for the BRIWECS dataset for each environment. Shaded areas represent standard errors.

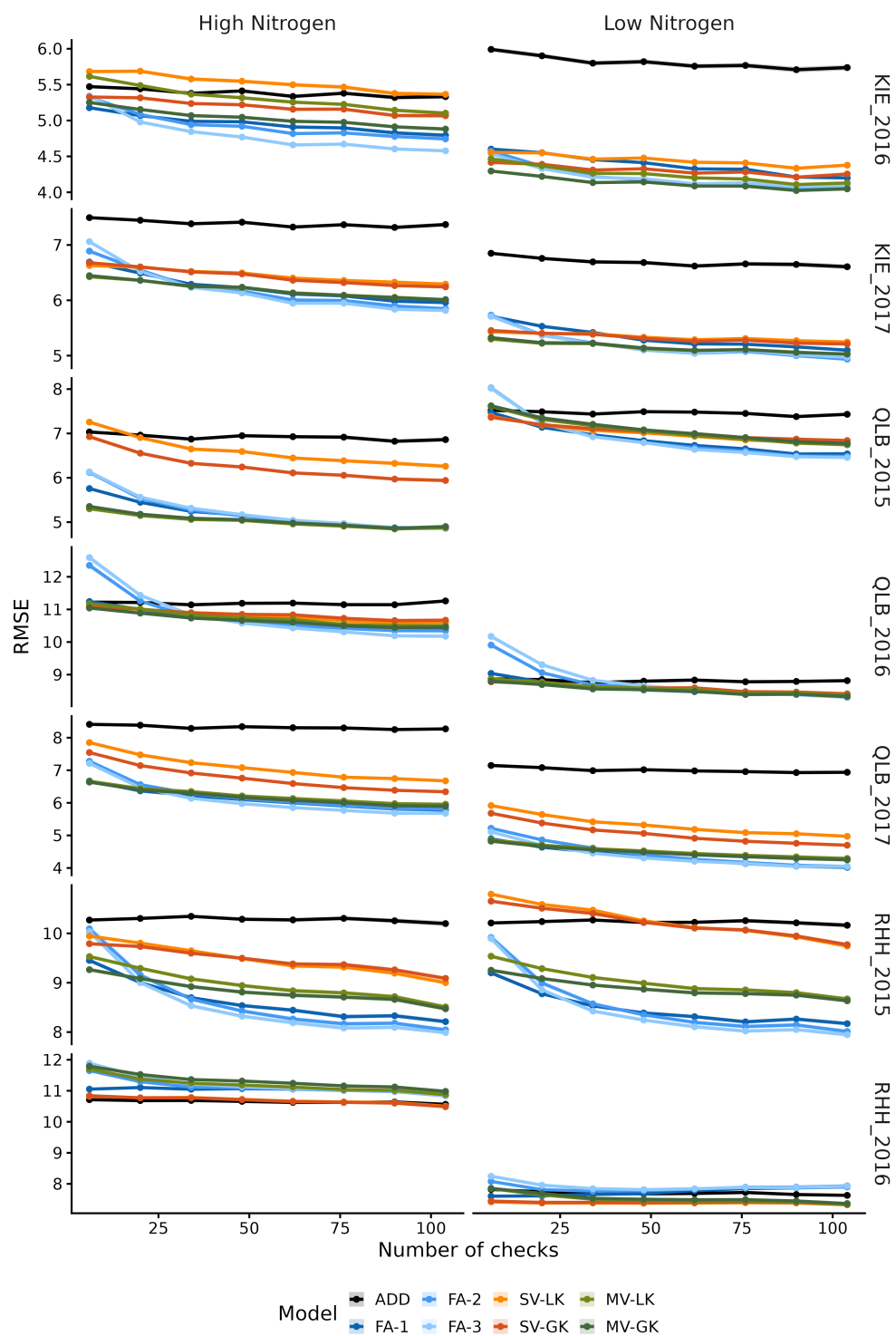


FIGURE S6. Continued. RMSE between BLUPs from the LMMs and centered test-set phenotypes for the BRIWECS dataset for each environment. Shaded areas represent standard errors.

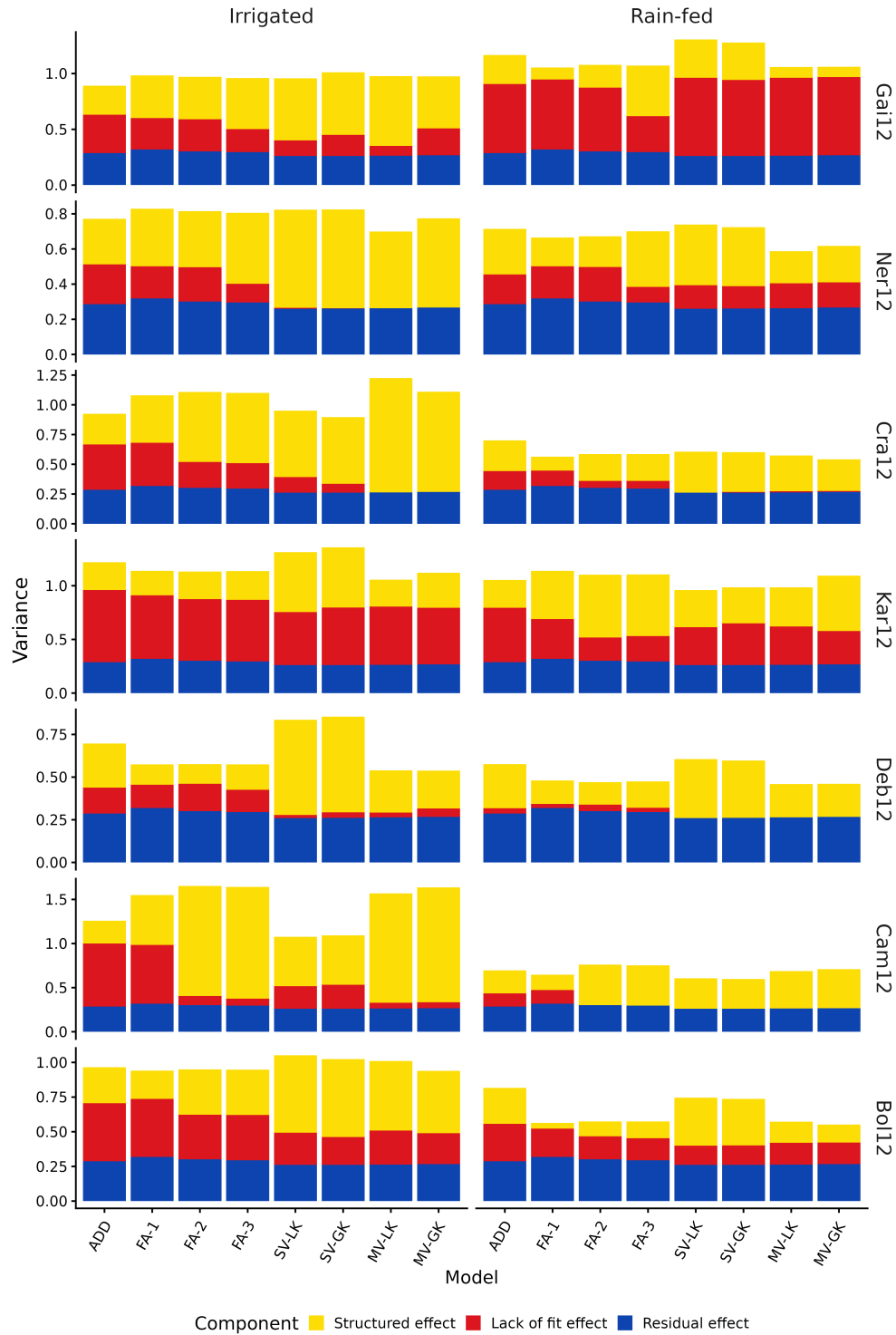


FIGURE S7. Partitioning of $G \times E \times M$ variance into structured, lack of fit, and residual effects for each environment in the DROPS dataset.

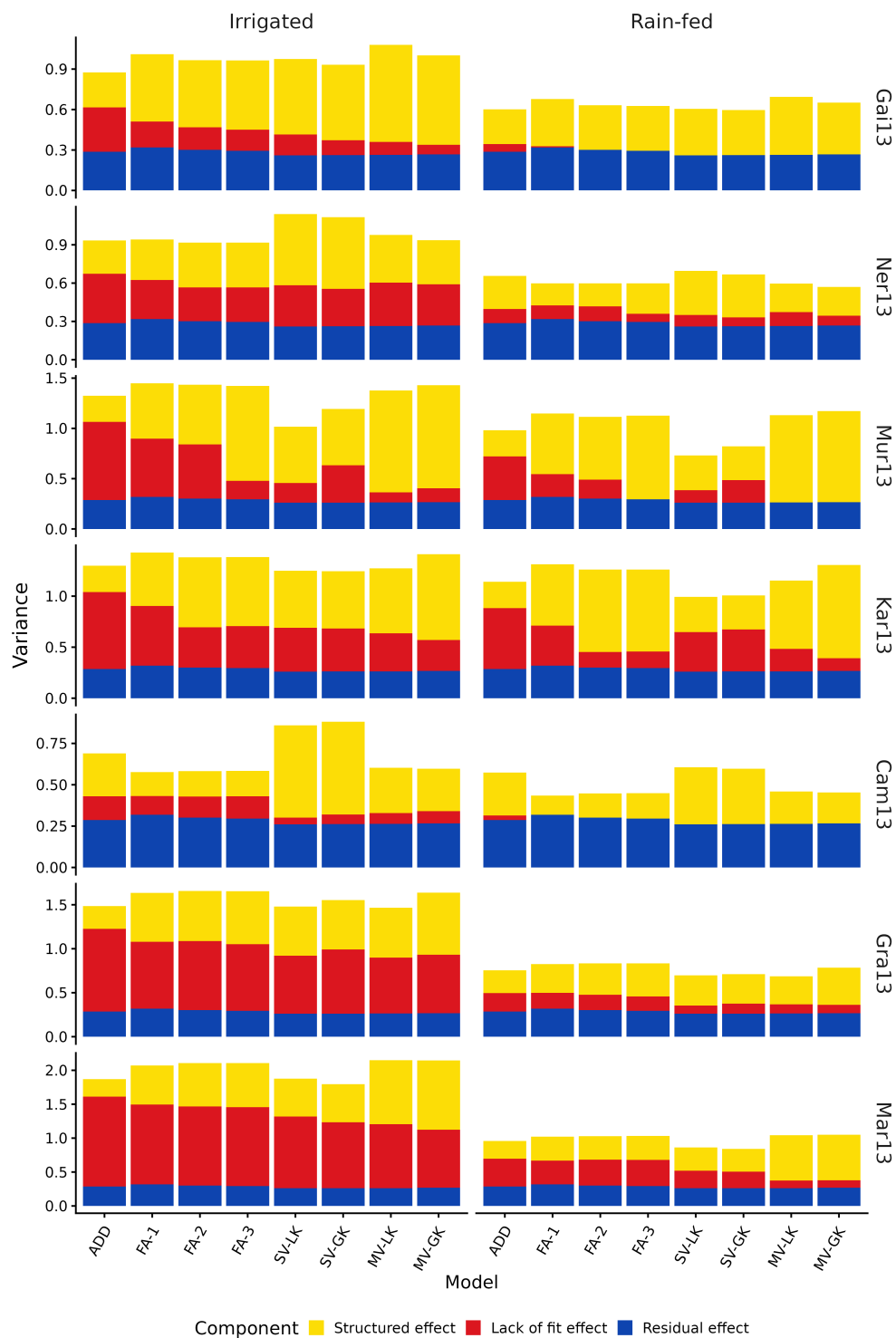


FIGURE S8. Continued. Partitioning of $G \times E \times M$ variance into structured, lack of fit, and residual effects for each environment in the DROPS dataset.

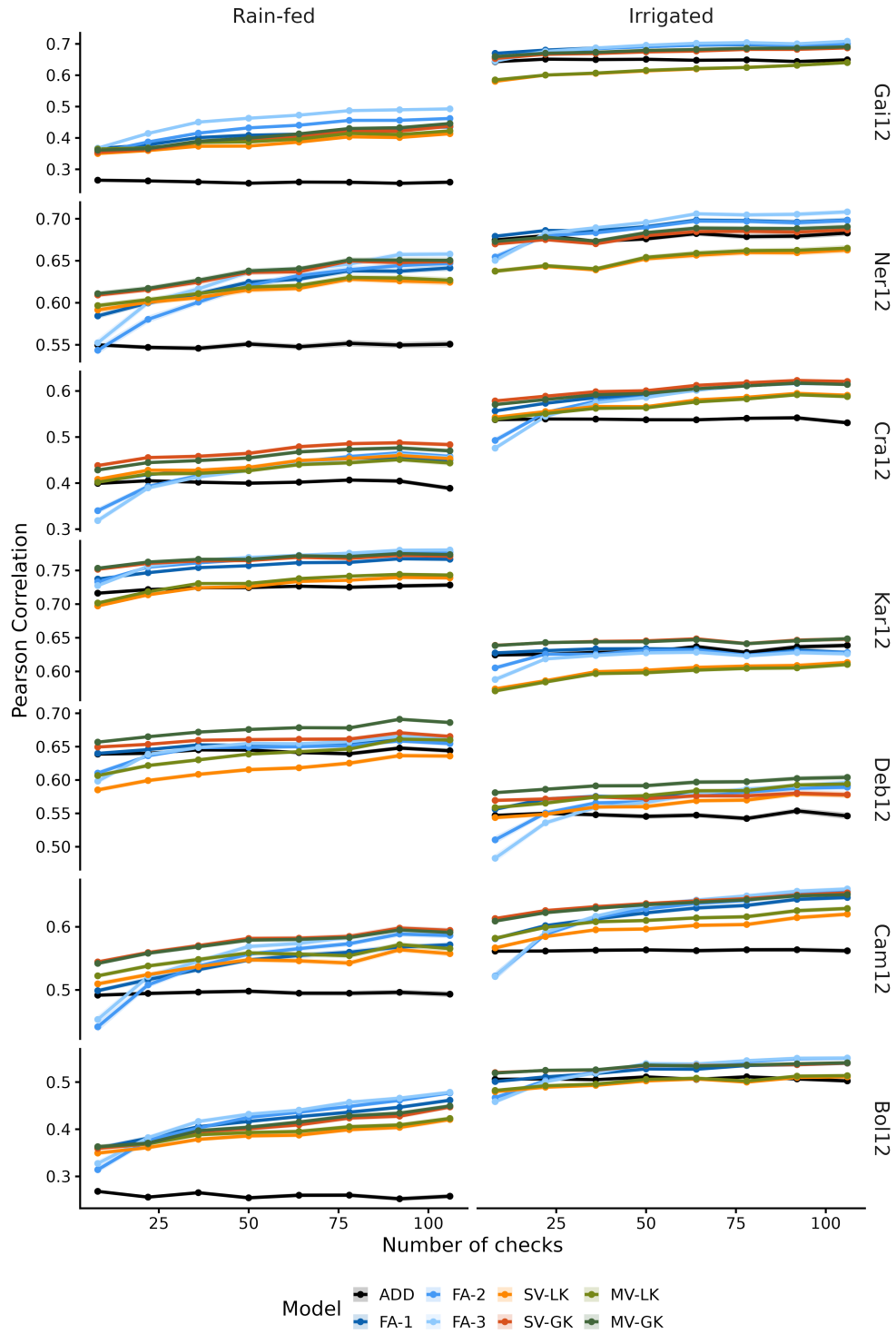


FIGURE S9. Pearson correlation between BLUPs from the LMMs and centered test-set phenotypes for the DROPS dataset for each environment. Shaded areas represent standard errors.

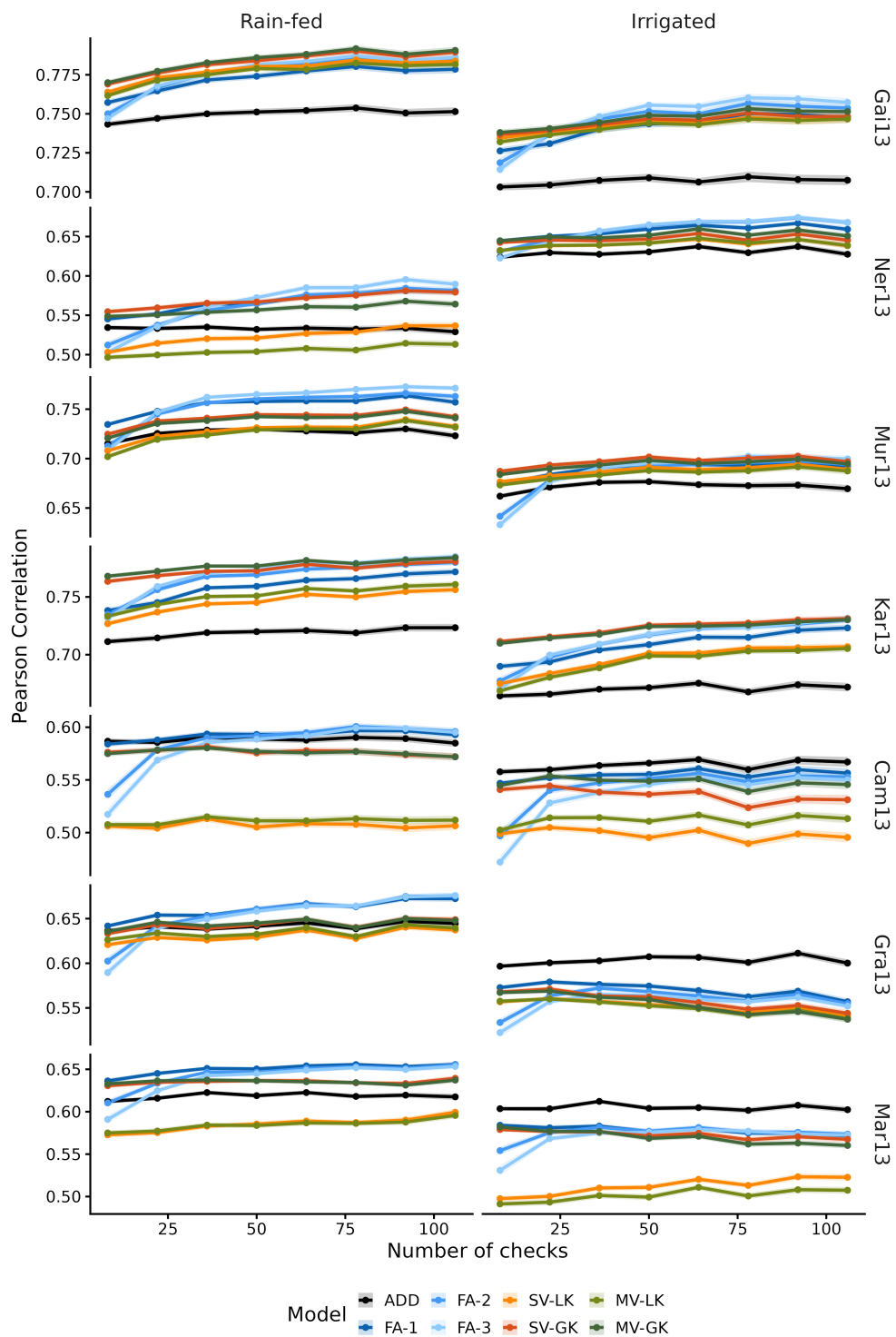


FIGURE S10. Continued. Pearson correlation between BLUPs from the LMMs and centered test-set phenotypes for the DROPS dataset for each environment. Shaded areas represent standard errors.

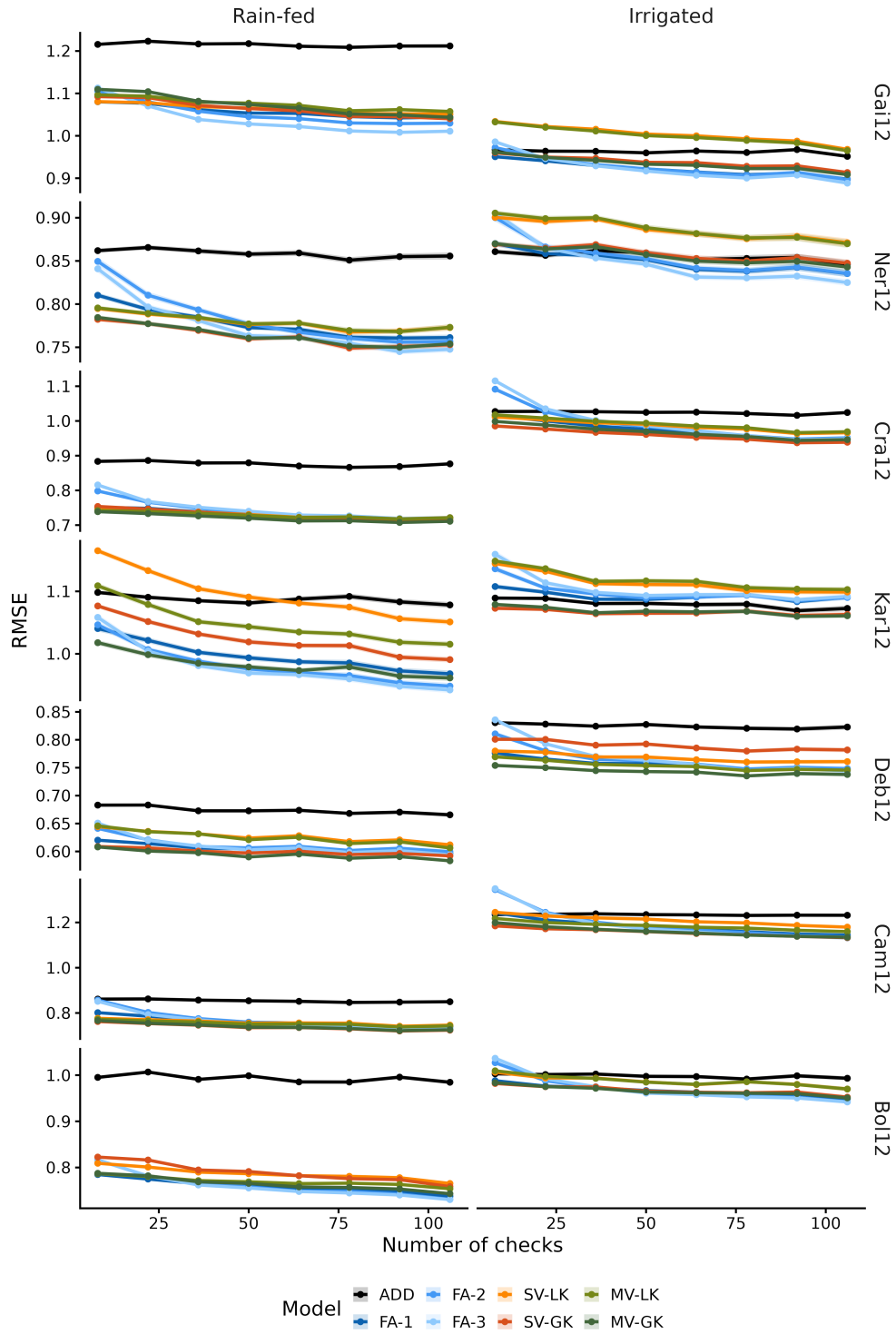


FIGURE S11. RMSE between BLUPs from the LMMs and centered test-set phenotypes for the DROPS dataset for each environment. Shaded areas represent standard errors.

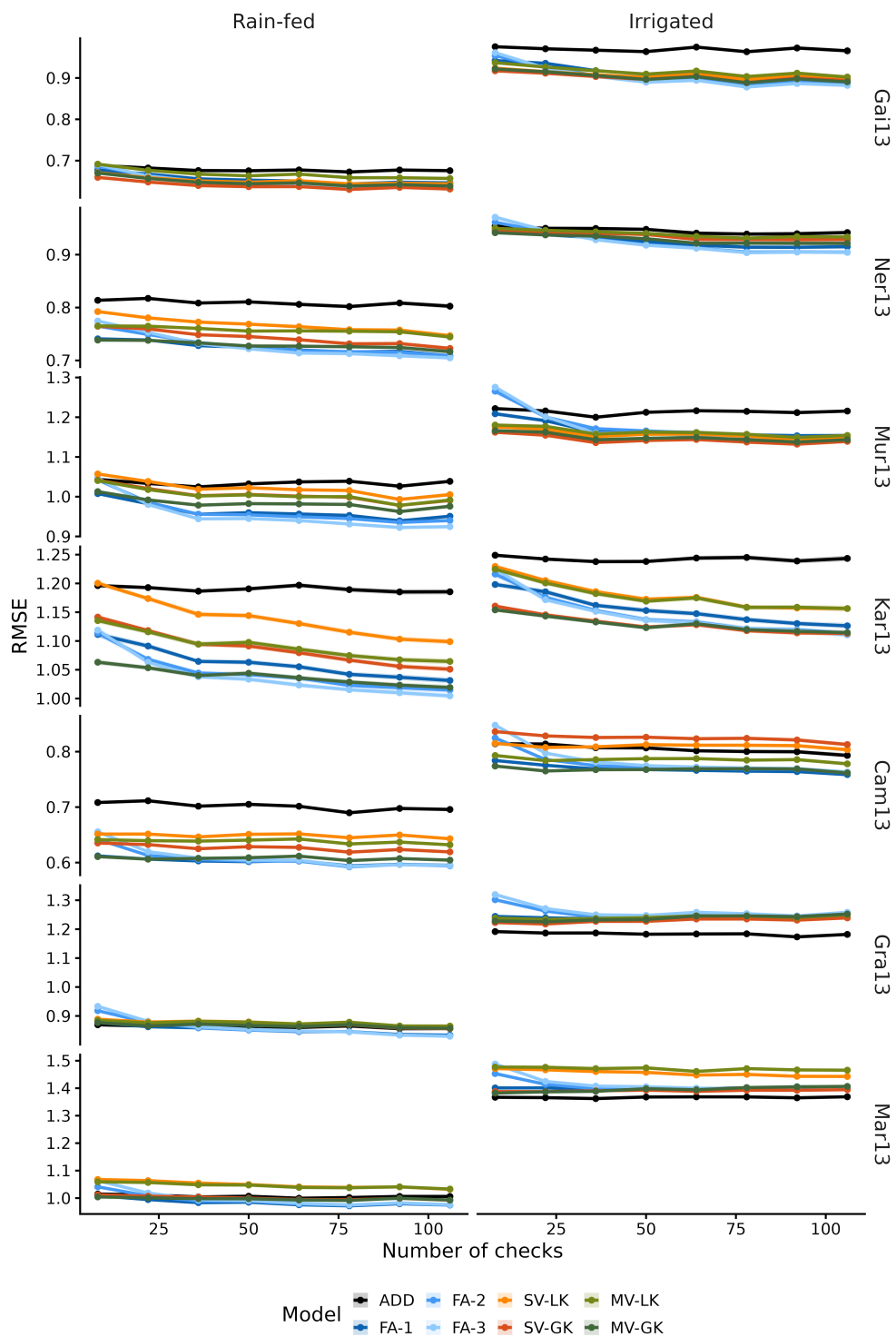


FIGURE S12. Continued. RMSE between BLUPs from the LMMs and centered test-set phenotypes for the DROPS dataset for each environment. Shaded areas represent standard errors.